

UCD-99-23
IFT-99-31
hep-ph/0003091
 March, 2000

How Valuable is Polarization at a Muon Collider? A Test Case: Determining the CP Nature of a Higgs Boson

Bohdan Grzadkowski^{1 a)} **John F. Gunion**^{2 b)} and **Jacek Pliszka**^{1 c)}

¹ *Institute of Theoretical Physics, Warsaw University, Warsaw, Poland*

² *Davis Institute for High Energy Physics, UC Davis, CA, USA*

Abstract

We study the use of polarization asymmetries at a muon collider to determine the CP-even and CP-odd couplings of a Higgs boson to $\mu^+ \mu^-$. We determine achievable accuracy as a function of beam polarization and luminosity. The appropriate techniques for dealing with the polarization precession are outlined. Strategies especially appropriate for a two-Higgs-doublet model (including the MSSM) are given. Our general conclusion is that polarization will be very useful, especially if the proton source is such that full luminosity in the storage ring can be retained even after imposing cuts on the originally accepted muons necessary for $P \gtrsim 0.4$ for each beam.

^{a)}E-mail:bohdang@fuw.edu.pl

^{b)}E-mail:jfgucd@physics.ucdavis.edu

^{c)}E-mail:pliszka@fuw.edu.pl

1 Introduction

Although the origin of mass has still not been established, it is widely expected that electroweak symmetry breaking is driven by elementary scalar dynamics, leading to one or more physical Higgs bosons [1]. It is also very possible that CP violation arises either partially or entirely as result of CP violation in the Higgs sector [2]. Even if not, CP violation in other sectors of the theory can induce CP violation in the Higgs sector at the loop level [3]. Thus, we anticipate that the direct determination of the CP nature of each observed Higgs boson could be crucial to unraveling the nature of the full theory.

Even if the minimal one-doublet Standard Model turns out to be nature's choice, we will certainly want to know that the single observed Higgs boson is entirely CP-even in nature. Alternatively, if electroweak symmetry breaking turns out to be driven by technicolor-like dynamics, it would be highly desirable to be able to check that the narrow, light pseudo-Nambu-Goldstone bosons (PGB's), that often arise in such a theory and are rather Higgs-like in many respects (see, for example, [4]), do indeed have CP-odd coupling to fermions.

The means for determining the CP nature of an observed narrow resonance are limited. If it is determined that its WW or ZZ coupling is substantial (small), then we will know that it has a substantial (small) CP-even component. But, even in the general two-Higgs-doublet model the relation between this coupling and the CP-even and CP-odd fermionic couplings (denoted a and $ib\gamma_5$, respectively, in $\bar{f}(a + ib\gamma_5)f^{\dagger 1}$) is model-dependent. However, polarization correlations can allow one to extract the ratio b/a in a model independent manner. For a light resonance, one possibility is to employ the $\tau^+\tau^-$ decay of the resonance. If the $t\bar{t}$ mode is open, then it too can be employed. These final-state possibilities were examined for a muon collider in [5, 6]. One can also look for certain characteristic angular distributions in associated production, $b\bar{b}$ +resonance or $t\bar{t}$ +resonance, that are sensitive to b/a [7]. However, the most elegant approach to determining the CP nature of a neutral resonance is to employ initial state polarization asymmetries. This is possible only for $\gamma\gamma$ [8] or $\mu^+\mu^-$ [6, 9] production of the resonance. But, the $\gamma\gamma$ coupling of a neutral resonance is the result of either loop(s) (in the Higgs case) or an anomaly (in the PGB case), and is not a direct measure of the elementary fermionic couplings. This leaves $\mu^+\mu^-$ collisions, which are also the only way in which we will probe 2nd generation fermionic couplings in models where the strength of the fermionic coupling is proportional to the fermion mass (implying that a resonance with mass $> 2m_\tau$ will always decay to 3rd generation fermions and any CP-odd coupling to two photons will be dominated by the top quark loop).

In the limit of $\beta_\mu = \sqrt{1 - 4m_\mu^2/m_R^2} \rightarrow 1$, the cross section for production of a

^{#1}Phases can always be chosen so that, for any given f , a and b are real.

resonance, R , with $\overline{\mu}(a + ib\gamma_5)\mu$ coupling to the muon takes the form

$$\begin{aligned}\overline{\sigma}_S(\zeta) &= \overline{\sigma}_S^0 \left(1 + P_L^+ P_L^- + P_T^+ P_T^- \left[\frac{a^2 - b^2}{a^2 + b^2} \cos \zeta - \frac{2ab}{a^2 + b^2} \sin \zeta \right] \right) \\ &= \overline{\sigma}_S^0 \left[1 + P_L^+ P_L^- + P_T^+ P_T^- \cos(2\delta + \zeta) \right],\end{aligned}\quad (1)$$

where $\delta \equiv \tan^{-1} \frac{b}{a}$ and P_T (P_L) is the degree of transverse (longitudinal) polarization^{#2} of each of the beams defined as $P \equiv f^+ - f^-$, with f^+ being the fraction of muons with spin in the dominant direction and f^- the fraction of muons with opposite spin. Here, ζ is the angle of the μ^+ transverse polarization relative to that of the μ^- as measured using the the direction of the μ^- 's momentum as the \hat{z} axis. The S subscript denotes ‘signal’. Both the $\cos \zeta$ and $\sin \zeta$ dependences allow significant sensitivity to the ratio of interest, b/a , even though only the $\sin \zeta$ term is truly CP-violating. The value of $\overline{\sigma}_S^0$, which results from convoluting the resonance shape with a Gaussian distribution in \sqrt{s} , depends upon the model, the detector, the final state mode and the machine parameters. Ignoring final state efficiencies and acceptance cuts, and integrating over final state phase space, one finds [9] a result that can be approximated by^{#3}

$$\overline{\sigma}_S^0 = \frac{4\pi\Gamma(R \rightarrow \mu^+\mu^-)BR(R \rightarrow F)}{m_R^2\Gamma_R^{\text{tot}} \left[1 + \frac{8}{\pi} \left(\frac{\sigma_{\sqrt{s}}}{\Gamma_R^{\text{tot}}} \right)^2 \right]^{1/2}}, \quad (2)$$

where $\sigma_{\sqrt{s}}$ is the Gaussian resolution in \sqrt{s} .

It is expected that the muon collider will first be operated with the relatively small natural polarization of $P \sim 0.2$ for the μ^+ and μ^- bunches, since this will allow maximal machine luminosity and lead to the largest number of Higgs events. The bunch polarizations will be oriented in the plane of the final storage ring so that their precession as the muon bunches circulate (for roughly 1000 turns) can be used to precisely determine the central energies of the muon bunches and their Gaussian energy spread [11, 12]. (One measures the oscillations of the energies of the electrons from the decaying muons, which oscillations depend very sensitively upon both the muon energy and the Gaussian energy spread.) From Eq. (1) and the fact that $|P_L^+ P_L^-|$ and $|P_T^+ P_T^-|$ are both ≤ 0.04 , it is clear that these observations will, to an excellent approximation, provide a measurement of $\overline{\sigma}_S^0$. (By choosing appropriate relative phases between the μ^+ and μ^- polarization angles, the polarization dependent terms in Eq. (1) will average to zero — see the next section.) Thus, a very accurate measurement of $\overline{\sigma}_S^0$ in several channels F can be performed and a reasonably accurate measurement of Γ_R^{tot} by a three-point scan

^{#2}Note that the cross section for longitudinally polarized muons depends only on $a^2 + b^2$ and cannot be used to extract information about the CP nature of the resonance's couplings to muons.

^{#3}This form, from Ref. [10], has the correct asymptotic limits for $\Gamma_R/\sigma_{\sqrt{s}} \rightarrow 0$ and $\Gamma_R/\sigma_{\sqrt{s}} \rightarrow \infty$ and is always within 18% of the exact result.

will be possible. A model-independent determination of $a^2 + b^2$ then becomes possible from Eq. (2) by computing $\Gamma(R \rightarrow \mu^+ \mu^-)$ using the measured values of $\bar{\sigma}_S^0$, Γ_R^{tot} , and $\sigma_{\sqrt{s}}$ and a determination of $BR(R \rightarrow F)$. To obtain $BR(R \rightarrow F)$ requires using the missing mass technique in the ZR final state (in either $e^+ e^-$ or $\mu^+ \mu^-$ collisions) to measure $\sigma(ZR \rightarrow ZX)$ ($X = \text{anything}$) and the measurement of $\sigma(ZR \rightarrow ZF)$ to compute $BR(R \rightarrow F) = \sigma(ZR \rightarrow ZF)/\sigma(ZR \rightarrow ZX)$. Once the basic Higgs observations have been performed so that the Higgs width, branching ratios and $a^2 + b^2$ are well-determined, the next task will be to perform a model-independent measurement of b/a . This requires maximizing the influence of the polarization-dependent terms in Eq. (1). Determining the best procedure for doing so and estimating the accuracy with which this measurement can be carried out is the main goal of this paper.

Any given final state F will have a significant background. In general, the cross section for the background is nearly independent of $\sigma_{\sqrt{s}}$. If we integrate over final state configurations then the background is independent of P_T^+ and P_T^- and ζ . In order to roughly understand the level of sensitivity to b/a that can be achieved, let us for the moment imagine that we can set $P_L^+ = P_L^- = 0$ and choose $P_T^+ = P_T^- = P_T$. We then denote the integrated background cross section by $\bar{\sigma}_B^0$. We imagine isolating $\frac{a^2-b^2}{a^2+b^2}$ and $\frac{-2ab}{a^2+b^2}$, respectively, via the asymmetries

$$\mathcal{A}_I \equiv \frac{\bar{\sigma}_S(\zeta = 0) - \bar{\sigma}_S(\zeta = \pi)}{\bar{\sigma}_S(\zeta = 0) + \bar{\sigma}_S(\zeta = \pi)} = P_T^2 \frac{a^2 - b^2}{a^2 + b^2} = P_T^2 \cos 2\delta, \quad (3)$$

$$\mathcal{A}_{II} \equiv \frac{\bar{\sigma}_S(\zeta = \pi/2) - \bar{\sigma}_S(\zeta = -\pi/2)}{\bar{\sigma}_S(\zeta = \pi/2) + \bar{\sigma}_S(\zeta = -\pi/2)} = -P_T^2 \frac{2ab}{a^2 + b^2} = -P_T^2 \sin 2\delta. \quad (4)$$

Assuming that $(a^2 + b^2)$ must be measured at the same time as the asymmetries, the error for the measurement of either of the asymmetries \mathcal{A}_I or \mathcal{A}_{II} is given by

$$[\delta \mathcal{A}]^2 = \frac{\bar{\sigma}_S^0 + \bar{\sigma}_B^0 + \mathcal{A}^2 (\bar{\sigma}_B^0 - \bar{\sigma}_S^0)}{L [\bar{\sigma}_S^0]^2} \quad (5)$$

where L is the integrated collision luminosity, assumed distributed equally between the two ζ measurements and we have temporarily taken P_T to be the same for all collisions (which is not actually the case, as will be discussed shortly). If $(a^2 + b^2)$ has already been very accurately determined using initial resonance production measurements and the technique outlined below Eq. (2), then the expression for $[\delta \mathcal{A}]^2$ takes the form

$$[\delta \mathcal{A}]^2 = \frac{\bar{\sigma}_S^0 + \bar{\sigma}_B^0 - \mathcal{A}^2 [\bar{\sigma}_S^0]^2 (\bar{\sigma}_S^0 + \bar{\sigma}_B^0)^{-1}}{L [\bar{\sigma}_S^0]^2} \quad (6)$$

In either case, if $P_T < 0.5$, and since $\mathcal{A}^2 \leq P_T^4$, the \mathcal{A}^2 in the numerator of $[\delta \mathcal{A}]^2$ can be neglected, implying that $\frac{\mathcal{A}^2}{[\delta \mathcal{A}]^2}$ is proportional to $P_T^4 L$.

From this discussion, it is apparent that the ideal situation would be to arrange for the muons to be entirely transversely polarized at the interaction point (IP)

and to be able to adjust the angle between the μ^- and μ^+ polarizations to be fixed at one of the four values $\zeta = 0, \pi/2, \pi, 3\pi/2$ for each collision. However, this is not possible if we are interested in a very narrow resonance, such as a light SM-like Higgs boson which will have a width of just a few MeV. The reasons follow. First, it is important to note that without intervention any horizontal (i.e perpendicular to the magnetic field of the storage ring) polarization will precess about the magnetic field and therefore rotate relative to the momentum direction. Consequently, the amounts of transverse and longitudinal polarization at the time the bunch passes the IP will oscillate. This will be described in more detail in the following section. The only way to overcome this oscillation would be to have a section of the storage ring devoted to compensating for this spin precession on a turn-by-turn basis. However, this conflicts with the requirement that we be able to measure the central energy of each muon bunch circulating in the storage ring to 1 part in 10^6 (and the beam energy spread of the bunch to better than 1 part in 10^2) using measurements of the oscillations of the energy of the secondary electrons from the muon decays as the bunches circulate and their spins precess. A large number of turns in which the precession is allowed to occur without compensation is required. The above precisions are those needed for a light Higgs resonance with a SM-like width (of a few MeV) in order to be certain of remaining rather precisely centered on the resonance peak and knowing exactly how that resonance peak is being sampled. For a resonance with width of a few hundred MeV or larger, knowledge of the beam energies to 1 part in 10^4 would be adequate. Since magnetic fields would be known and be stable at this level, direct measurement of the bunch energies would not be required and one could consider turn-by-turn spin compensation so as to achieve the ideal transverse configurations at the IP for each collision. Here, we will assume that the storage ring will not initially be built with the extra magnetic components required for such compensation.

Thus, regardless of whether the Higgs or other resonance is broad or narrow, it is necessary to determine the effects of spin precession on the accuracy with which $\cos 2\delta$ and $\sin 2\delta$ can be determined. In what follows, we develop a procedure whereby the luminosity needed to achieve a given accuracy is only about 50% larger when the spins are allowed to precess than if the spins could be taken to be purely transverse for each collision.

2 Polarization Precession at a Muon Collider

Most muon collider designs are such that there are two bunches, each, of μ^+ 's and μ^- 's circulating in opposite directions in the storage ring. Typically, these bunches will be stored for about 1000 turns. Once the bunches enter the storage ring, any polarization in the horizontal plane will precess in the vertical magnetic field of the storage ring. Further, as noted in the introduction, for the case of a very narrow resonance this precession is needed to measure the bunch energies and Gaussian

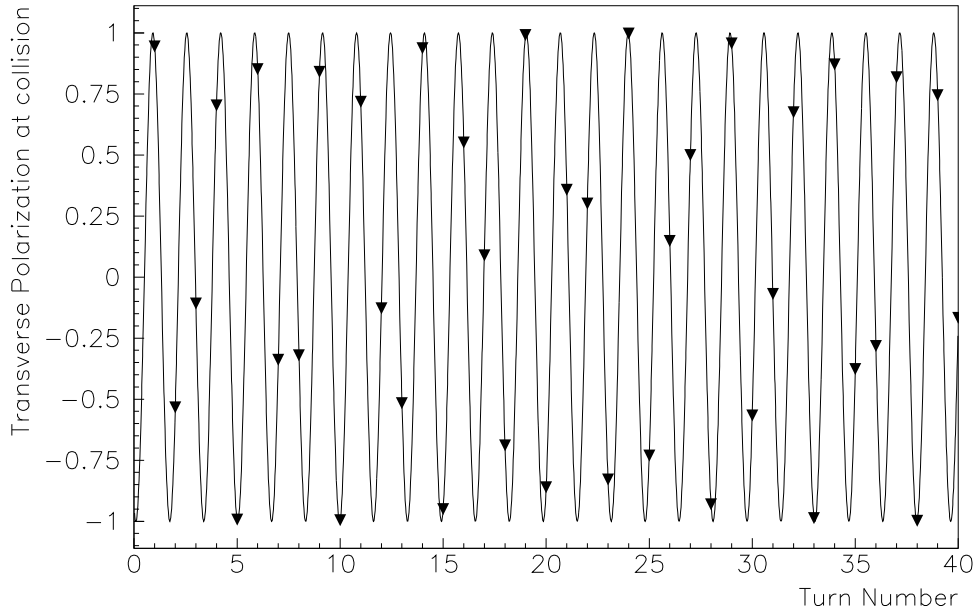


Figure 1: We plot $P_H^\perp(N_T)/|\vec{P}_H|$ at the interaction point as a function of the number of times, N_T , that the μ^- beam passes the IP, assuming the muon collider is operating at a total center of mass energy of $\sqrt{s} = 110$ GeV and that the μ^- enters the storage ring with longitudinal polarization $P_H^\parallel/|\vec{P}_H| = 1$. This plot is from [14].

spreads to high accuracy, implying that the polarizations of the bunches should not be manipulated once they are stored in the ring. The impact of such precession on extracting physics has not been carefully examined to date. Thus, we provide in this section a fairly detailed explanation of the considerations and procedures that must be employed. Even though we shall focus on the case of a narrow spin-0 resonance, the general features of our discussion will have wider applicability.

The typical configuration will be such that a given bunch enters the ring with a component \vec{P}_V (\vec{P}_H) of polarization vertical (horizontal) with respect to the plane of the storage ring. [\vec{P}_V and \vec{P}_H are defined in the muon rest frame; see Eqs. (7) and (8) below.] \vec{P}_H^- and \vec{P}_H^+ will rotate in the same directions as the μ^- and μ^+ themselves (that is in opposite directions). The rate of rotation of the \vec{P}_H 's as viewed from the laboratory frame is somewhat different than the rate at which the bunches themselves rotate. The mismatch means that if, for instance, \vec{P}_H^- were longitudinal at the time the μ^- bunch first enters the storage ring, it will not remain so but rather it will precess into the transverse direction and then back to the opposite longitudinal direction, and so forth.

To be precise, we assume that the storage ring's magnetic field points in the $-\hat{y}$ direction: $\vec{B} = -B\hat{y}$. The μ^- is then rotating clockwise about the \hat{y} axis. At any given moment, we define $\hat{z} = \hat{p}_{\mu^-}$. Then, \hat{x} points radially outward. The angle θ^- is defined as the angle by which one must rotate (in the μ^- rest frame) about the \hat{y} axis in order to get from \hat{z} to \vec{P}_H^- ; θ^- is an 'over-rotation' angle in that it is the additional angle of rotation of the spin as compared to the angle of rotation of \vec{p}_{μ^-} . After boosting to the laboratory frame, the complete four-component spin vector for the μ^- is then:

$$s_{\mu^-} = P_H^- [\gamma(\beta, \hat{z}) \cos \theta^- - (0, \hat{x}) \sin \theta^-] + P_V^-(0, \hat{y}). \quad (7)$$

The standard result of Ref. [13], assuming that the μ^- beam enters the storage ring with $\hat{P}_H^- = \hat{p}_{\mu^-}$, is $\theta^-(N_T) = \omega(N_T - 1/2)$, where N_T is the number of turns during storage, counted starting with $N_T = 1$ the first time the bunch passes the IP ($N_T = 1/2$ at bunch insertion), and $\omega = 2\pi\gamma\frac{g_{\mu^-}-2}{2}$, with $\gamma = E/m_\mu$ and $\frac{g_{\mu^-}-2}{2} = 1.165924 \times 10^{-3}$. One finds that $\omega = \pi$ for a beam energy of 90.6223 GeV/2 (i.e. close to $m_Z/2$), implying that an initially longitudinal μ^- horizontal polarization becomes transverse after the μ^- travels half way around the ring to the interaction point. However, for the somewhat higher energies of interest for a Higgs factory, the degree of horizontally transverse polarization (denoted by \perp) oscillates with N_T according to $P_H^\perp(N_T)/|\vec{P}_H| = \sin \theta^-(N_T)$ as illustrated in Fig. 1, where we have chosen a convention in which P_H^\perp is positive when it points towards the center of the storage ring. We now discuss how to take this oscillation into account.

First, we note that similar results apply for the μ^+ . The μ^+ will be traveling in a counter-clockwise direction about the \hat{y} axis; *at the interaction point 1/2 way around the ring*, $\hat{p}_{\mu^+} = -\hat{z}$. Once again, we can define an over-rotation angle θ^+ (in the μ^+ rest frame), in terms of which the μ^+ 's spin vector (in the laboratory frame) at the interaction point is written as

$$s_{\mu^+} = P_H^+ [\gamma(\beta, -\hat{z}) \cos \theta^+ - (0, \hat{x}) \sin \theta^+] + P_V^+(0, \hat{y}). \quad (8)$$

If we start with $\hat{P}_H^+ = \hat{p}_{\mu^+}$ at the time of insertion, then $\theta^+(N_T) = \omega(N_T - 1/2)$, just as for $\theta^-(N_T)$. More generally, we can insert the μ^+ beam with any initial angle for \hat{P}_H^+ that we desire.

We assume that each time a Higgs event is observed we can compute, or will have measured (prior to the IP, and then extrapolated to the IP), the transverse polarizations of the bunches. That is, we will know θ^- and θ^+ for each interaction. In fact, θ^+ will be completely correlated with θ^- , the correlation being determined by the initial spin configuration with which the bunches are injected into the storage ring. We now give the expression for the cross section as a function of θ^- and θ^+ , defining $c_- \equiv \cos \theta^-$ etc.,

$$\begin{aligned} \frac{\sigma_S(\theta^+, \theta^-)}{\sigma_S^0} = & (1 + P_H^+ P_H^- c_+ c_-) + \cos 2\delta (P_V^+ P_V^- + P_H^+ P_H^- s_+ s_-) \\ & + \sin 2\delta (P_H^- P_V^+ s_- - P_H^+ P_V^- s_+). \end{aligned} \quad (9)$$

Note that we obtain Eq. (1) using the obvious replacements: $P_H^+ c_+ = P_L^+$, $P_H^- c_- = P_L^-$, $P_V^+ P_V^- + P_H^+ P_H^- s_+ s_- = P_T^+ P_T^- \cos \zeta$, and $P_H^- s_- P_V^+ - P_H^+ s_+ P_V^- = -P_T^+ P_T^- \sin \zeta$. We also note that if we choose $P_V^+ = P_V^- = 0$ and insert the bunches so that $\theta^+ = \theta^- + \pi/2$, then all polarization dependent terms in Eq. (9) average to zero after many turns. This is the configuration that would normally be employed for the initial Higgs resonance scans so that knowledge of b/a would not be needed in order to properly interpret these measurements.

However, to determine b/a we will wish to employ one or more different polarization configurations and retain maximum information by binning Higgs events according to $(\theta^-, \theta^+(\theta^-))$. After integrating over (θ, ϕ) configurations in an $f\bar{f}$ final state, one finds (in the limit of $m_f/\sqrt{s} \rightarrow 0$)

$$\begin{aligned} \sigma_B(\theta^-, \theta^+) \propto & e_f^2 e_\mu^2 (1 - P_H^+ P_H^- c_+ c_-) \Pi_\gamma^2 \\ & + 2e_f e_\mu c_f \left[c_\mu ((1 - P_H^+ P_H^- c_+ c_-) + d_\mu (P_H^- c_- - P_H^+ c_+)) \right] \Pi_\gamma \Re(\Pi_Z) \\ & + (c_f^2 + d_f^2) \left[(c_\mu^2 + d_\mu^2) (1 - P_H^+ P_H^- c_+ c_-) + 2c_\mu d_\mu (P_H^- c_- - P_H^+ c_+) \right] |\Pi_Z|^2, \end{aligned} \quad (10)$$

where the γ , Z propagators and couplings are Π_γ and Π_Z and ie_f and $i\gamma_\mu (c_f + d_f \gamma_5)$, respectively; see the Appendix for more details.

In order to give a simplified discussion, let us assume that $\bar{\sigma}_S^0$ (and, thence, $a^2 + b^2$) has been precisely determined by first resonance production measurements that do not focus on determining the Higgs CP properties. As we have described in the introduction, this is very likely to be the case. Then, remembering that θ^+ can be considered to be a function of θ^- for any given choice of storage ring insertion configuration, we can write the signal cross section as

$$\bar{\sigma}_S^C(\theta^-) = f_0^C(\theta^-) + \cos 2\delta f_c^C(\theta^-) + \sin 2\delta f_s^C(\theta^-), \quad (11)$$

where

$$\begin{aligned} f_0^C(\theta^-) &= \bar{\sigma}_S^0 (1 + P_H^+ P_H^- c_+ c_-), \\ f_c^C(\theta^-) &= \bar{\sigma}_S^0 (P_V^+ P_V^- + P_H^+ P_H^- s_+ s_-), \\ f_s^C(\theta^-) &= \bar{\sigma}_S^0 (P_H^- P_V^+ s_- - P_H^+ P_V^- s_+) \end{aligned} \quad (12)$$

depend upon the configuration, C , chosen for $P_H^+, P_H^-, P_V^+, P_V^-, \theta^+(\theta^-)$. (Recall that $\theta^+(\theta^-)$ is determined by the choice made for the relative angle between the polarization of the μ^+ as compared to that of the μ^- at the time of bunch insertion.) The assumption that $a^2 + b^2$ has been precisely determined already corresponds to assuming that $f_0^C(\theta^-)$ is completely known. Then, writing $\Sigma^C(\theta^-) \equiv \bar{\sigma}_S^C(\theta^-) + \bar{\sigma}_B^C(\theta^-)$, the $\Delta\chi^2$ difference between two different Higgs models with the same $a^2 + b^2$ but different values of δ will be given by

$$\Delta\chi^2 = \sum_C L_C \left[\Delta_c^2 M_{cc}^C + 2\Delta_c \Delta_s M_{cs}^C + \Delta_s^2 M_{ss}^C \right], \quad (13)$$

where L_C is the luminosity devoted to configuration C ,

$$M_{cc}^C = \int \frac{d\theta^-}{2\pi} \frac{[f_c^C(\theta^-)]^2}{\Sigma^C(\theta^-)} \quad M_{cs}^C = \int \frac{d\theta^-}{2\pi} \frac{[f_c^C(\theta^-)f_s^C(\theta^-)]}{\Sigma^C(\theta^-)} \quad M_{ss}^C = \int \frac{d\theta^-}{2\pi} \frac{[f_s^C(\theta^-)]^2}{\Sigma^C(\theta^-)}, \quad (14)$$

and we have defined $\Delta_c \equiv \Delta \cos 2\delta$ and $\Delta_s \equiv \Delta \sin 2\delta$ (the differences in these two quantities between the two models).^{#4} The θ^- integral is over the value of θ^- (and the correlated $\theta^+(\theta^-)$ value) at the interaction point. Here, we are approximating the sum over the discrete θ^- values that arise during the course of 1000 turns of the bunches by an integral over θ^- . This is an excellent approximation unless $\sqrt{s}/90.62 \text{ GeV}$ (where 90.62 GeV is the \sqrt{s} value such that θ^- is constant) is a ratio of small (compared to 1000) integers.

We will demonstrate below that the configurations can be chosen sufficiently cleverly that one can neglect the θ^- , and, indeed, the entire configuration dependence of $\Sigma^C(\theta^-)$ and approximate $\Sigma^C(\theta^-) \sim \bar{\sigma}_S^0 + \bar{\sigma}_B^0$, the sum of the unpolarized cross sections. Under these circumstances, the $\Delta\chi^2$ for discriminating between two different models with the same $a^2 + b^2$ value (i.e. same total unpolarized rate) will then be given by

$$\Delta\chi^2 = \frac{[\bar{\sigma}_S^0]^2}{\bar{\sigma}_S^0 + \bar{\sigma}_B^0} \sum_C L_C \hat{\mathcal{S}}_C^2, \quad (15)$$

where

$$\hat{\mathcal{S}}_C^2 = \left\langle \left[\Delta_c (P_V^+ P_V^- + P_H^+ P_H^- s_+ s_-) + \Delta_s (P_H^- P_V^+ s_- - P_H^+ P_V^- s_+) \right]^2 \right\rangle_C \quad (16)$$

is a measure of our ‘sensitivity’ to $\cos 2\delta$ and $\sin 2\delta$. The averaging is over roughly 1000 turns of the bunches in the storage ring. To an excellent approximation, this average depends only on the relative values of θ^+ and θ^- at the time of bunch insertion. We will now give results for $\hat{\mathcal{S}}^2$ for (a) $\theta^- = \theta^+$ (b) $\theta^- = \theta^+ + \pi$ (c) $\theta^- = \theta^+ + \pi/2$. The result for (d) $\theta^- = \theta^+ + 3\pi/2$ is the same as for (c). We find

$$\begin{aligned} \hat{\mathcal{S}}_a^2 &= \Delta_c^2 \left[\frac{3}{8} (P_H^+ P_H^-)^2 + P_H^+ P_H^- P_V^+ P_V^- + (P_V^+ P_V^-)^2 \right] + \frac{1}{2} \Delta_s^2 \left[P_H^+ P_V^- - P_H^- P_V^+ \right]^2, \\ \hat{\mathcal{S}}_b^2 &= \Delta_c^2 \left[\frac{3}{8} (P_H^+ P_H^-)^2 - P_H^+ P_H^- P_V^+ P_V^- + (P_V^+ P_V^-)^2 \right] + \frac{1}{2} \Delta_s^2 \left[P_H^+ P_V^- + P_H^- P_V^+ \right]^2, \\ \hat{\mathcal{S}}_c^2 &= \Delta_c^2 \left[\frac{1}{8} (P_H^+ P_H^-)^2 + (P_V^+ P_V^-)^2 \right] + \frac{1}{2} \Delta_s^2 \left[(P_H^+ P_V^-)^2 + (P_H^- P_V^+)^2 \right]. \end{aligned} \quad (17)$$

We note that $M_{cs} = 0$ when the θ^- dependence of Σ^C is neglected.

As noted earlier in the previous section, the ideal situation would be to be able to choose four basic relative orientations of the μ^- and μ^+ transverse polarizations

^{#4}We note that in the limit of just two bins corresponding to $\sin \zeta = \pm 1$ or $\cos \zeta = \pm 1$, $\Delta\chi^2 = 1$ corresponds to errors for $\sin 2\delta$ or $\cos 2\delta$, respectively, as given in Eq. (6).

with respect to each other: $\zeta = 0, \pi/2, \pi, 3\pi/2$. Constant $\zeta = 0$ or $\zeta = \pi$ could be accomplished by setting $P_H^+ = P_H^- = 0$ and $P_V^+ = P_V^-$ or $P_V^+ = -P_V^-$, respectively. However, as noted in the previous section, some degree of horizontal precessing polarization is necessary if we are to be able to measure the energies of the muon bunches with the accuracy of 1 part in 10^6 needed for a very narrow Higgs resonance. It is estimated that $P_H^+ = P_H^- \sim 0.05 - 0.1$ [14] is required for the energy measurement. (We will adopt the optimistic choice of 0.05 in the remainder of this paper.) The rest can be placed in the vertical directions.

The spin precessions make it impossible to maintain $\zeta = \pi/2$ or $\zeta = 3\pi/2$ as the bunches circulate. The simplest thing that one can do is to inject, say, the μ^- bunches with purely horizontal polarization, and maximize the vertical polarization for the μ^+ bunches subject to the requirement that $P_H^+ = 0.05$. Sensitivity to both the magnitude and sign of $\sin 2\delta$ arises from the variation of the $\sin 2\delta P_H^- s_- P_V^+$ term in Eq. (16), which at various extremes samples $\zeta = \pi/2$ and $\zeta = 3\pi/2$. (We again emphasize the importance of either calculating, starting from the insertion configuration, or measuring, from the decay spectrum, the precession angles associated with each observed Higgs event.)

Very specifically, we thus consider the following configurations, keeping in mind that the net polarization P for the μ^+ and μ^- bunches will be essentially the same.

I: To approximate the $\zeta = 0$ configuration, we choose $P_H^+ = P_H^- = P_H = 0.05$, $\theta^- = \theta^+$, $P_V^+ = P_V^- = \sqrt{P^2 - P_H^2}$. The sensitivity is then given by

$$\hat{\mathcal{S}}_I^2 = \hat{\mathcal{S}}_a^2 = \Delta_c^2 \left[3P_H^4/8 + P_H^2(P^2 - P_H^2) + (P^2 - P_H^2)^2 \right]. \quad (18)$$

II: To approximate the $\zeta = \pi$ configuration, we choose $P_H^+ = P_H^- = P_H = 0.05$, $\theta^- = \theta^+ + \pi$, $P_V^- = -P_V^+ = -\sqrt{P^2 - P_H^2}$. The sensitivity is then given again by Eq. (18): $\hat{\mathcal{S}}_{II}^2 = \hat{\mathcal{S}}_I^2$.

We now justify, for the case of $C = I, II$, the approximation of taking $\Sigma^C \sim \bar{\sigma}_S^0 + \bar{\sigma}_B^0$, employed in obtaining Eq. (15) from Eqs. (13) and (14). We note that for both configuration I and configuration II the background, see Eq. (10), will depend only very weakly on (θ^-, θ^+) simply because P_H^- and P_H^+ are both small. Similarly, the $P_H^+ P_H^- c_+ c_-$ term in $f_0^C(\theta^-)$ and the $P_H^+ P_H^- s_+ s_-$ term in $f_c^C(\theta^-)$ will be very small. Further, $f_s^C(\theta^-)$ can be approximately neglected because both P_H^+ and P_H^- are small. Finally, we will sum over configurations I and II (with equal luminosity weighting) in order to determine $\cos 2\delta$. This has the important consequence that (using $|P_V^\pm| \simeq P$, see above) the leading P^4 term in Eq. (18) is obtained from Eqs. (13) and (14) via the structure

$$\begin{aligned} \sum_{C=I,II} M_{cc}^C &\sim P^4 [\bar{\sigma}_S^0]^2 \left(\frac{1}{\bar{\sigma}_B^0 + \bar{\sigma}_S^0 (1 + P^2 \cos 2\delta)} + \frac{1}{\bar{\sigma}_B^0 + \bar{\sigma}_S^0 (1 - P^2 \cos 2\delta)} \right) \\ &= P^4 [\bar{\sigma}_S^0]^2 \left(\frac{2(\bar{\sigma}_B^0 + \bar{\sigma}_S^0)}{(\bar{\sigma}_B^0 + \bar{\sigma}_S^0)^2 - P^4 \cos^2 2\delta (\bar{\sigma}_S^0)^2} \right), \end{aligned} \quad (19)$$

so that even for P as large as 0.5 or so (as we shall later consider) the P^4 correction term in the denominator can be neglected.^{#5} Thus, the approximation of taking $\Sigma^C \sim \bar{\sigma}_S^0 + \bar{\sigma}_B^0$ is quite accurate in this case.

III: To emphasize the $\zeta = \pi/2$ and $\zeta = 3\pi/2$ configurations over many turns of the bunches, we choose $P_H^- = P$ ($P_V^- = 0$), $P_H^+ = P_H = 0.05$ and $P_V^+ = \sqrt{P^2 - P_H^2}$. In addition, we choose $\theta^- = \theta^+ + \pi/2$ (or $\theta^- = \theta^+ + 3\pi/2$) so as to minimize dependence on Δ_c . The sensitivity is then given by

$$\hat{\mathcal{S}}_{III}^2 = \hat{\mathcal{S}}_c^2 = \frac{1}{8} \Delta_c^2 P^2 P_H^2 + \frac{1}{2} \Delta_s^2 P^2 (P^2 - P_H^2). \quad (20)$$

Note that if we choose either $\theta^- = \theta^+$ or $\theta^- = \theta^+ + \pi$, then the (undesired) sensitivity to Δ_c would be increased. For $P_H \leq 0.05$ and $P > 0.2$ (as will be the case), the Δ_c^2 term can be dropped in Eq. (20).

In order to justify neglecting the dependence of Σ^C on θ^- in case III, we note that the terms of concern in $\sigma_B(\theta^-, \theta^+)$, Eq. (10), are those proportional to $(P_H^- c_- - P_H^+ c_+) \sim P c_-$. The term of concern in $\sigma_S(\theta^-, \theta^+)$ is that proportional to $f_s(\theta^-) \sim \bar{\sigma}_S^0 P^2 s_-$. We will return to this latter term in a moment. First, we note that the $P c_-$ term in $\sigma_B(\theta^-, \theta^+)$ can be approximately eliminated without affecting $\sigma_S(\theta^-, \theta^+)$ by binning together into a single c_-^0 bin events with the same sign of s_- but with $c_- = c_-^0$ and $c_- = -c_-^0$. (Even after 1000 turns, this is only an approximation since the number of turns for which $c_- \sim c_-^0$ can differ significantly from the number of turns for which $c_- \sim -c_-^0$, depending upon the Higgs boson mass and the number of c_- bins employed.) Concerning the $\sigma_S(\theta^-, \theta^+)$ term proportional to $P^2 s_-$, we note that in computing M_{ss} , Eq. (14), the leading term in the numerator is even in s_- while the $P^2 s_-$ correction term in the $\sigma_S(\theta^-, \theta^+)$ contribution to Σ^C is odd. This means that we will get a cancellation analogous to that in Eq. (19) so that these corrections to our approximation will be of relative order P^4 and can be neglected.

It is useful to note how these results compare to the ideal where we imagine that ζ can be held fixed. For $\zeta = 0, \pi$, our sensitivity $\hat{\mathcal{S}}^2$ would be $\Delta_c^2 P^4$ while for $\zeta = \pi/2, 3\pi/2$ it would be $\Delta_s^2 P^4$. For $P_H = 0.05$ we suffer a loss of about 0.469 (0.939) for Δ_s (Δ_c) for $P = 0.2$ and 0.495 (0.990) for $P = 0.5$. In the remainder of this paper, we approximate these $P_H = 0.05$ results by assuming no loss in $\hat{\mathcal{S}}^2$ for Δ_c and a factor of 1/2 loss in $\hat{\mathcal{S}}^2$ for Δ_s . This latter factor must be overcome by increased luminosity to obtain the same statistical accuracy as in the ideal case. To equalize sensitivity to Δ_s and Δ_c , we will assume that we accumulate twice as much luminosity for the Δ_s configurations as for the Δ_c configurations. Thus, for total integrated luminosity L we accumulate $L/6$ in configuration I, $L/6$ in configuration II, and $2L/3$ in configuration III. Of the latter $2L/3$, as the spins

^{#5}Note the analogy to Eq. (6) that is apparent when we recall that $|\delta A|^2$ corresponds to $\Delta\chi^2 = 1$ and that \mathcal{A}^2 in the present case is $P^4 \cos^2 2\delta$.

precess $L/3$ will be accumulated in configurations with $\sin \zeta < 0$ and $L/3$ with $\sin \zeta > 0$. The sensitivity achieved is then equivalent to probing the four fixed ζ configurations ($\zeta = 0, \pi/2, \pi, 3\pi/2$) with $L/6$ each. The results of the following sections will sometimes be phrased in this latter language.

3 Maximizing Sensitivity to CP Violation

The number and density of muons in each bunch are limited by space-charge and muon beam power considerations. Existing designs have proton source intensity such that these limits are saturated when momentum cuts on the initially accepted muons coming from the target are such that the muon beams have polarization of $P \sim 0.2$ (or less). To date, there has been no strong reason for designing the proton source so as to have full luminosity (fully saturated bunches) for larger P values. This is because the typical design for the storage ring is such that the polarization is longitudinal at the interaction point half way around the ring, motivated by the fact that (for longitudinal P) the signal rate is proportional to $1 + P^2$, while γ^*, Z^* induced (e.g. $b\bar{b}$) backgrounds are proportional to $1 - P^2$. In this configuration, the improvement of $S/\sqrt{S + B}$ with increasing P (assuming the integrated luminosity can be kept fixed) is rather slow, rising by $\lesssim 20\%$ from $P = 0.2$ to $P = 0.4$. Thus, although higher (longitudinal) P would have some advantage if the proton intensity were such that the two muon bunches were both fully saturated at $P \gtrsim 0.4$ rather than at $P \sim 0.2$, it is usually accepted that this advantage is not sufficient to justify the expense associated with building a more intense proton source.

However, if determining the CP nature of the resonance's couplings to $\mu^+ \mu^-$ is the goal, the (approximate) proportionality of the $\hat{\mathcal{S}}^2$ sensitivity measures (see previous section) to P^4 implies that retaining maximal luminosity at $P \gtrsim 0.4$ has much greater advantages. The extra proton source intensity required to achieve this is determined by the fraction, $f_{\text{surv}}(P)$, of muons that survive after imposing the momentum cuts required to achieve a certain P (prior to inserting the muon bunches into the storage ring). The variation of f_{surv} as a function of P has been estimated by many different groups (see, e.g., [11, 12]). Here, we adopt the post-cooling result given in [11] (Fig. 21) which is approximately described by $f_{\text{surv}}(P) = 1.45 - 2.51P$ for $0.2 \leq P \leq 0.6$. The number of muons in each bunch, N_b , is proportional to the proton source intensity, \mathcal{L}_{ps} , times f_{surv} . Using the specified form, one finds, for example, that $f_{\text{surv}}(0.45) : f_{\text{surv}}(0.39) : f_{\text{surv}}(0.2) \sim 1/3 : 1/2 : 1$, implying that \mathcal{L}_{ps} at $P = 0.45$ (0.39) must be 3 (2) times that for $P = 0.2$ to maintain full bunches.

If the machine is constructed with \mathcal{L}_{ps} only large enough to saturate the bunches at $P = 0.2$, then one finds that f_{surv} is such that $S/\sqrt{S + B}$ declines if one increases P above 0.2 (and arranges the polarization to be longitudinal at the interaction point). However, maximum $\hat{\mathcal{S}}$ is rather achieved by increasing P to the point ($P \sim 0.39$) where each muon bunch has one-half of the $P = 0.2$ number, N_b , and

then merging the two bunches into one bunch (prior to insertion into the storage ring). Bunch merging effectively doubles the storage ring luminosity at this P compared to what would result without bunch merging. (Without bunch merging, one would have luminosity proportional to $2 \times (N_b/2)^2$ whereas with bunch merging the luminosity would be proportional to $1 \times N_b^2$.) As a result, the collider luminosity at $P = 0.39$ is only a factor of 2 lower than at $P = 0.2$ and $P^2\sqrt{L}$ is roughly a factor of 2.7 larger. (At the same time, $S/\sqrt{S+B}$ has declined by about a factor of 1.4.) If CP studies are the goal, one will choose the $P = 0.39$ option with bunch merging. If \mathcal{L}_{ps} larger than that required to saturate the muon bunches at $P = 0.2$ is available, bunch merging may or may not be desirable for CP studies. For \mathcal{L}_{ps} such that bunch saturation is achieved for $P < 0.42$ (≥ 0.42), the sensitivity $\hat{\mathcal{S}}$ for CP studies will (will not) benefit by increasing P still further to the point where the bunches can be merged. If the bunch-merging option is appropriate, the integrated collider luminosity L will be one-half the (no merging) value at $P = 0.2$. If bunch saturation is the better option, L will be exactly the same as the $P = 0.2$ value. In either case, increasing P beyond the bunch saturation or bunch merging point (whichever is more optimal) causes $\hat{\mathcal{S}}$ to decline.

To be more explicit, we define the relative sensitivity $R_{\mathcal{S}} \equiv \hat{\mathcal{S}}/\hat{\mathcal{S}}_0$, where the denominator is that achieved using $P = 0.2$ and $\mathcal{L}_{\text{ps}}^0$ such that the two bunches are saturated for $P = 0.2$. Let us also define the relative source intensity $I \equiv \mathcal{L}_{\text{ps}}/\mathcal{L}_{\text{ps}}^0$. In Fig. 2, we plot $R_{\mathcal{S}}$ obtained either by bunch merging or bunch saturation (whichever gives the larger $R_{\mathcal{S}}$) as a function of I . Also shown is the corresponding polarization being employed as a function of I . The corresponding functional forms are: for bunch merging, $P^m(I) = a - \frac{b}{2I}$ with $R_{\mathcal{S}}^m(I) = \left(\frac{P^m(I)}{0.2}\right)^2 2^{-1/2}$; for simply filling two bunches, $P^f(I) = a - \frac{b}{I}$ with $R_{\mathcal{S}}^f(I) = \left(\frac{P^f(I)}{0.2}\right)^2$. Here, $a \simeq 0.577$ and $b \simeq 0.377$ for the form of f_{surv} given earlier. Below (above) $I = 2.38$ we employ P^m and $R_{\mathcal{S}}^m$ (P^f and $R_{\mathcal{S}}^f$). The results for $R_{\mathcal{S}}$ show clearly that if determining the CP nature of a resonance is the goal, then one gains by optimizing P and having as large a proton source intensity as is feasible.

Of course, the absolute accuracy with which a measurement of b/a can be made is dependent upon the resonance model. In the following section, we will consider several Higgs boson examples and demonstrate that by using optimal polarization, as described above, a very meaningful measurement of b/a can typically be performed. Overall, we will conclude that the increase in our ability to determine the CP nature of the muonic couplings of a resonance would provide substantial motivation for spare proton source intensity.

Before ending this section, we note that there is a very interesting possibility for increasing the number of muons with high polarization retained after making the necessary selection cuts. In particular [11, 15, 16], if the accelerating gradient of the phase-rotation device that immediately follows the pion capture solenoid is sufficiently high ($\sim 4 - 5$ MV/m), the correlation between the muon arrival time and average muon polarization might be significantly enhanced, resulting in a more

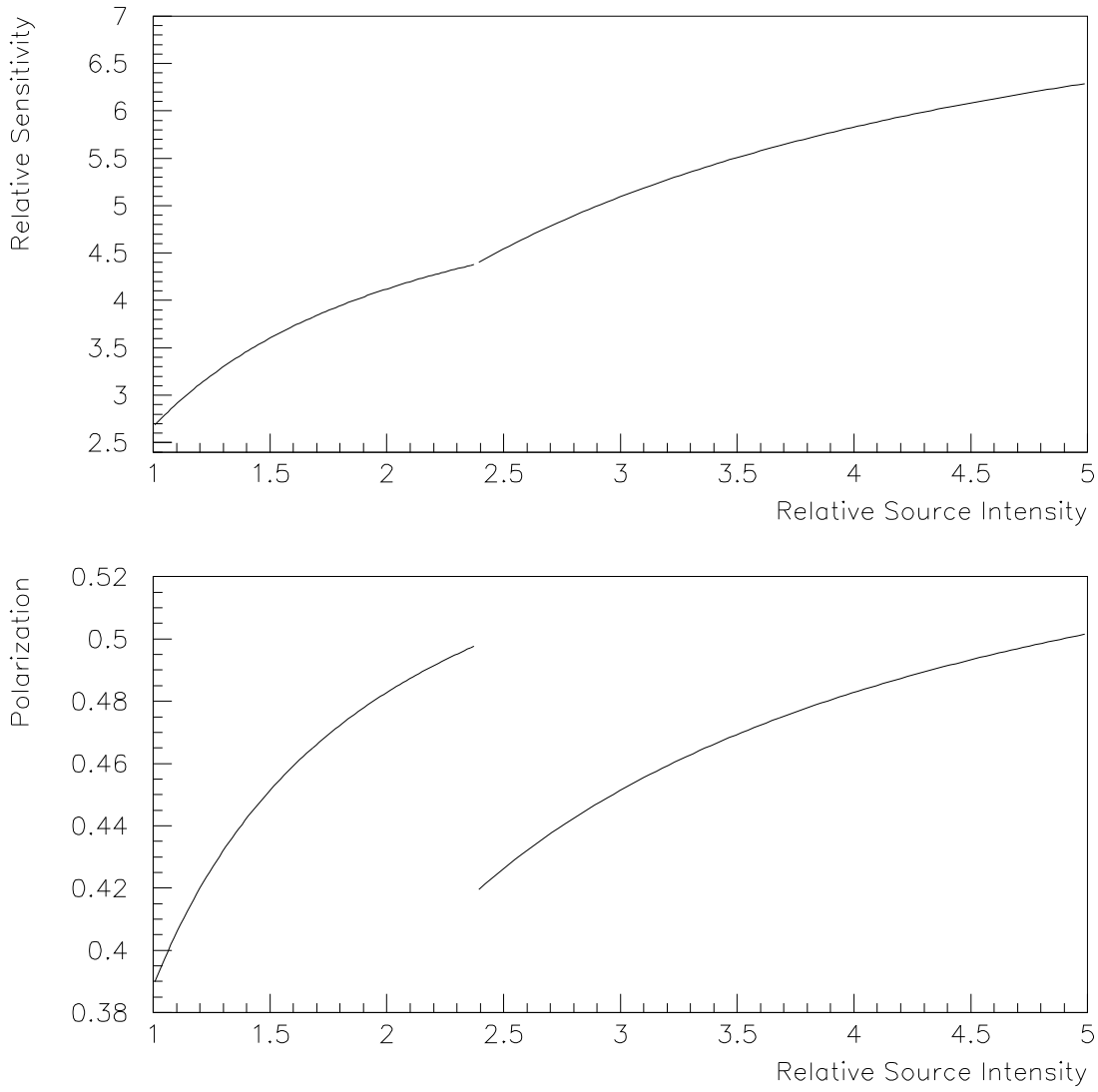


Figure 2: We plot the maximum achievable relative sensitivity R_S of the CP determination as a function of the relative proton source intensity I , both being relative to values corresponding to two full μ^+ and μ^- bunches (each) at $P = 0.2$. At $I = 2.38$, one switches from bunch merging to bunch filling. Also shown is the polarization being employed for a given I .

effective selection of polarized muons, and a higher final polarization for the same luminosity. Such high-gradient phase-rotation designs are being actively considered for the neutrino beam facility version of the muon accelerator and storage ring [16].

4 Two test cases: a light Higgs with SM-like $b\bar{b}$ rate and a degenerate H^0 – A^0 MSSM pair

Consider first the case of a Higgs boson with SM-like $b\bar{b}$ final state rate and total width. For example, it might be that a Higgs boson is detected and appears to have SM-like WW/ZZ couplings and branching ratios to accessible final states, in which case we will wish to determine if its fermionic couplings are indeed CP-even. Here, we assess the accuracy with which this verification can be performed at a muon collider. As detailed in earlier studies [9, 10], the result of Eq. (2) and the very small width of a light SM-like Higgs boson means that the muon collider must be operated with the smallest possible beam energy resolution, even if this results in substantial luminosity sacrifice. For currently understood designs, the best that can be achieved is $\Delta E_{\text{beam}}/E_{\text{beam}} \equiv R$ with R of order $R = 3 \times 10^{-5}$.^{#6} For such an R value, the yearly integrated luminosity is anticipated to be of order $L = 0.1 \text{ fb}^{-1}$ when the bunches are full. We will examine results achievable for $m_h = 110 \text{ GeV}$ and $m_h = 130 \text{ GeV}$ by employing only $F = b\bar{b}$.

The invariant amplitude squared for Higgs+ $\gamma^* + Z^*$ exchange is given in the Appendix as a function of the relative angle ζ between the transverse polarizations of the μ^- and μ^+ and as a function of both θ and ϕ , the angles describing the orientation of the b and \bar{b} momenta in the final state. We first note that the interference term is never of importance for the cases we explore here. Secondly, we observe that $|\mathcal{M}|^2$ from Higgs exchange is independent of θ and ϕ , whereas that for the $\gamma^* + Z^*$ background does depend upon both θ and ϕ . Our analysis proceeds as follows.

We assume input values for $(\hat{a}, \hat{b}) = (a, b)/(gm_\mu/2m_W)$ ($a \equiv a_\mu, b \equiv b_\mu$), denoting them by \hat{a}_0 and \hat{b}_0 . We integrate over ϕ , but bin events in $\cos \theta$ (bin label j). As described, the spin precession means that we must also bin events in θ^- (remembering that θ^+ will always have a known correlation with θ^- for a given spin-precession configuration); θ^- bins are labelled by i . We devote $L/6, L/6$ and $2L/3$ to the spin-precession configurations $C = I, II, III$ described in the previous section.^{#7} The number of events (including both signal and background) for a given configuration choice C , given θ^- bin i and given $\cos \theta$ bin j is denoted by $N(C, i, j)$. The statistical error for each such bin is $\Delta N(C, i, j) = \sqrt{N(C, i, j)}$. We

^{#6}In this paper, all R values will be quoted in absolute units and not in per cent.

^{#7}In all cases studied, if there are no a priori restrictions on the possible couplings, sensitivity to \hat{b}/\hat{a} is maximized by employing all the configurations.

then consider a different model characterized by \hat{a} and \hat{b} and compute

$$\Delta\chi^2 = \sum_{C,i,j} \frac{(N(C, i, j, \hat{a}, \hat{b}) - N(C, i, j, \hat{a}_0, \hat{b}_0))^2}{\Delta N^2(C, i, j, \hat{a}_0, \hat{b}_0)}. \quad (21)$$

The discussion of Section 2 shows that with appropriate binning and appropriate choices for our configurations we can effectively drop the C, i, j dependence of $\Delta N(C, i, j)$. The following discussion will implicitly rely on this fact.

The accuracy with which \hat{a} and \hat{b} can be determined can be assessed by drawing contours of constant $\Delta\chi^2$ in $\delta \equiv \tan^{-1} \hat{b}/\hat{a}$, $r \equiv \sqrt{\hat{a}^2 + \hat{b}^2}$ parameter space. The $n\sigma$ error in δ for example (which implicitly assumes that r is always adjusted for a given \hat{b}/\hat{a} so as to minimize the $\Delta\chi^2$) is given by drawing the vertical line tangent to the $\Delta\chi^2 = n^2$ contour. We will also include the $\Delta\chi^2 = 6.635$ contour corresponding to 99% CL. The corresponding statistical errors for $r \equiv \sqrt{\hat{a}^2 + \hat{b}^2}$ are obtained by the horizontal lines tangent to the contours. However, the true errors for r must incorporate the error coming from our imprecise knowledge of $BR(h \rightarrow b\bar{b})$ and Γ_h^{tot} .

Let us begin with the example of a SM Higgs boson ($\hat{a}_0 = 1$, $\hat{b}_0 = 0$) with mass $m_h = 110$ GeV. To illustrate the importance of polarization, we use as a reference point a total integrated luminosity at $P = 0.2$ (with full muon bunches) of $L = 0.15 \text{ fb}^{-1}$ (per year). We plot contours in (δ, r) parameter space for some sample cases: (i) $P = 0.2$, $I = 1$ (i.e. nominal proton source intensity, $\mathcal{L}_{\text{ps}}^0$); (ii) $P = 0.39$, $I = 1$ (bunch merging at $\mathcal{L}_{\text{ps}}^0$); (iii) $P = 0.48$, $I = 2$ (bunch merging at $\mathcal{L}_{\text{ps}} = 2\mathcal{L}_{\text{ps}}^0$); (iv) $P = 0.45$, $I = 3$ (full bunches at $\mathcal{L}_{\text{ps}} = 3\mathcal{L}_{\text{ps}}^0$). The contours are presented in Fig. 3. It is useful to keep in mind that $\hat{b}/\hat{a} = \tan \delta$ is 1 for $\delta = \pi/4 \sim 0.785$. For the cases (i)-(iv) above, the 1σ , 2σ , 99% CL, and 3σ limits on δ are: (i) $0.94, \dots$; (ii) $0.30, 0.64, 0.89, 1.14$; (iii) $0.20, 0.41, 0.53, 0.64$; and (iv) $0.15, 0.32, 0.42, 0.50$. The corresponding 1σ and 99% CL limits on $\hat{b}/\hat{a} = \tan \delta$ are: (i) $1.36, \dots$; (ii) $0.31, 1.23$; (iii) $0.20, 0.58$; (iv) $0.15, 0.45$. We see that even $I = 1$ with bunch merging gives a reasonable 1σ measurement; however, a good 99% CL limit on \hat{b}/\hat{a} requires $I \geq 2$.

Of course, as the Higgs mass increases, the event rates decline and the results worsen. This is illustrated in Fig. 4 which gives the same plots as Fig. 3, but for $m_h = 130$ GeV. Above $m_h = 130$ GeV, the $b\bar{b}$ branching ratio begins to decline sharply and one should see a significant WW^* final state rate, which in itself would be a signal of a significant CP-even component for the Higgs boson. A high discrimination check of the CP nature of the muonic coupling would be possible by including the WW^* channel in the transverse polarization analysis. We will not pursue this here.

Another perspective on our errors is to ask how well separated the \hat{b}/\hat{a} measurement for a SM Higgs boson is from the same measurement for an alternative Higgs boson of the general two-Higgs-doublet model (2HDM). To illustrate, consider $m_h = 110$ GeV with $\hat{a}_0 = \hat{b}_0 = \frac{1}{\sqrt{2}}$. The $\Delta\chi^2$ contours for this input model are

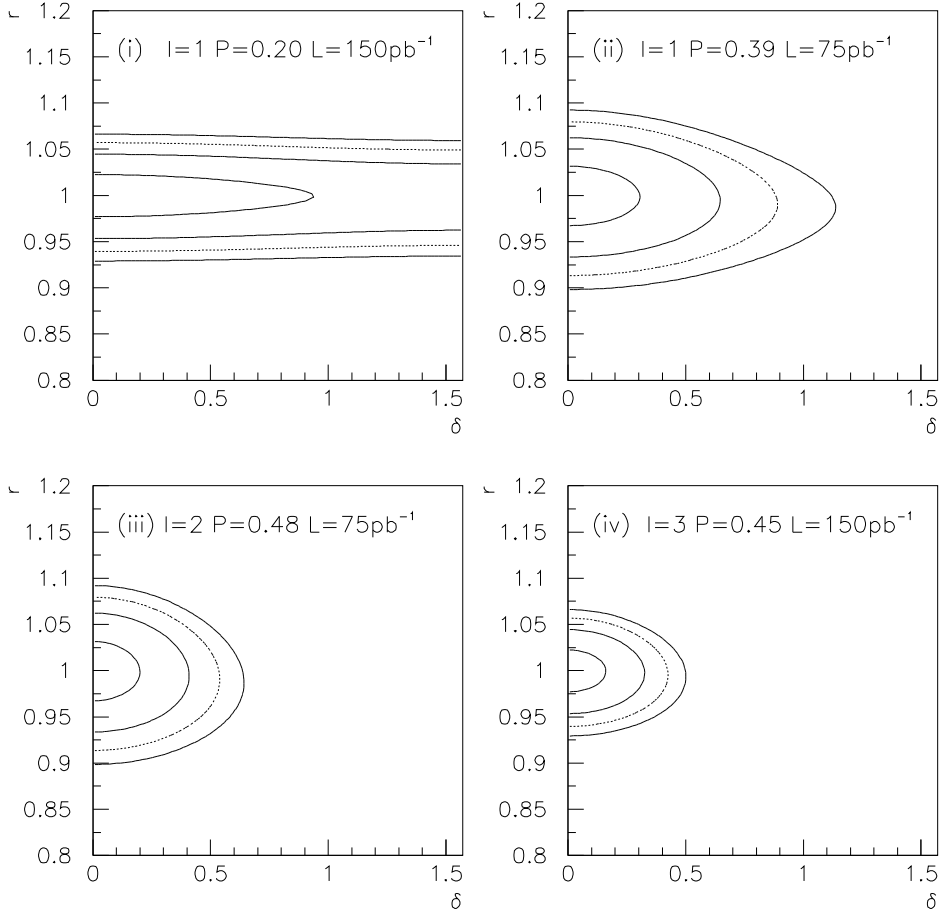


Figure 3: We give contours at $\Delta\chi^2 = 1, 4, 6.635, 9$ in the δ, r parameter space assuming that the integrated luminosity at polarization $P = 0.2$ (with full muon bunches) is $L = 0.15 \text{ fb}^{-1}$. Four cases are compared: (i) $P = 0.2$, $L = 0.15 \text{ fb}^{-1}$ (which corresponds to $I = 1$); (ii) maintaining same proton source intensity, $I = 1$, but merging the bunches, corresponding $P^m(I = 1) \sim 0.39$, for which $L = 0.075 \text{ fb}^{-1}$; (iii) increasing the proton source intensity by a factor of two, $I = 2$, while merging the bunches, corresponding to $P^m(I = 2) \sim 0.48$, for which $L = 0.075 \text{ fb}^{-1}$; (iv) $I = 3$, using just-full bunches, corresponding to $P^f(I = 3) \sim 0.45$, for which $L = 0.15 \text{ fb}^{-1}$. We assume a SM Higgs boson ($\hat{a}_0 = 1$, $\hat{b}_0 = 0$) with $m_h = 110 \text{ GeV}$ and an overall efficiency (including b -tagging efficiency) of 0.54.

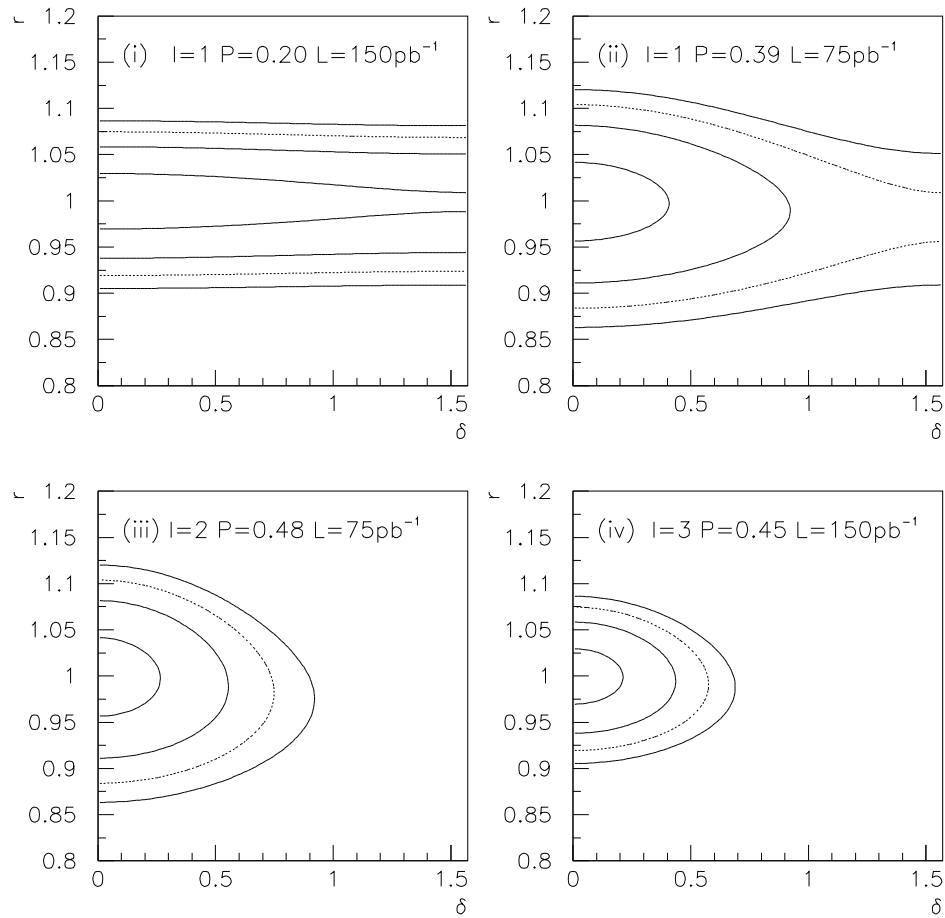


Figure 4: Same as Fig. 3, but for $m_h = 130 \text{ GeV}$.

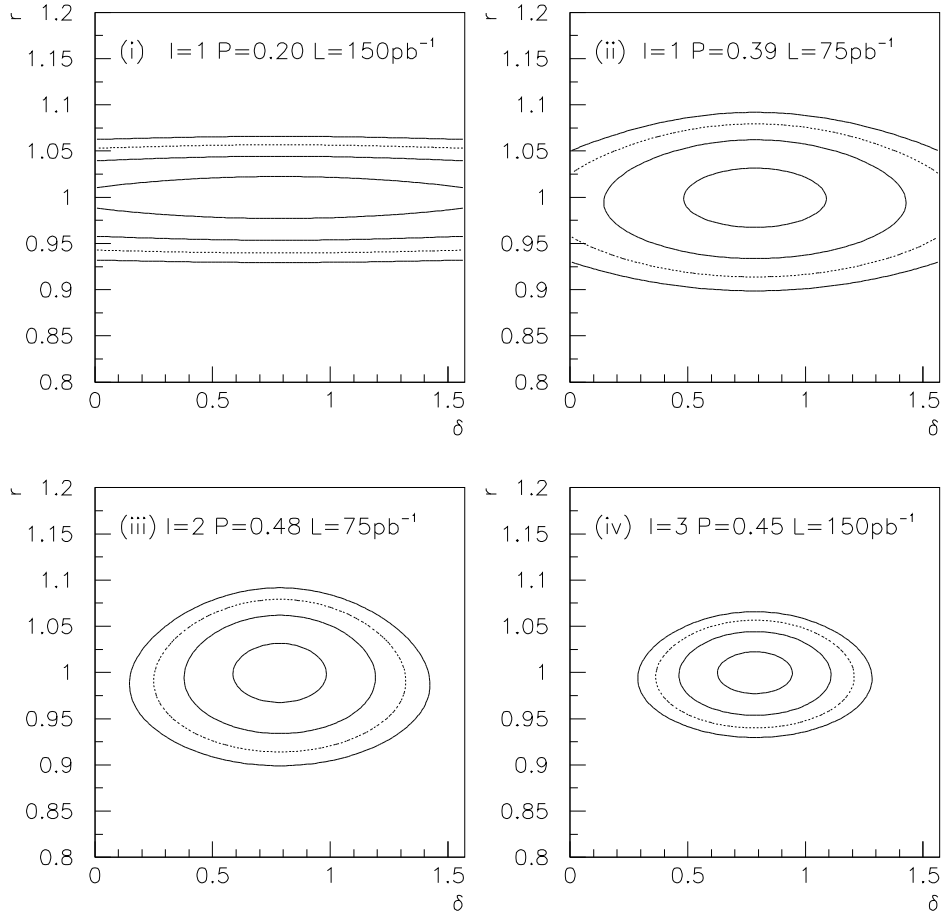


Figure 5: Same as Fig. 3, but for a mixed-CP higgs boson with $\hat{a}_0 = \hat{b}_0 = 1/\sqrt{2}$ and $m_h = 110 \text{ GeV}$.

given in Fig. 5. The 1σ contours are already non-overlapping with those for a pure CP-even Higgs (Fig. 3) for $P = 0.39$ and $I = 1$. However, the 99% CL contours have a small overlap even at $I = 3$ ($P = 0.45$). This again emphasizes the potential importance of larger-than-nominal source luminosity for such discrimination.

Table 1: Event number pattern for different Higgs models as a function of ζ , assuming $P_L^\pm = 0$ and $P_T^\pm = P$; see Eq. (1).

(\hat{a}, \hat{b})	$\zeta = 0$	$\zeta = \pi/2$	$\zeta = \pi$	$\zeta = 3\pi/2$
(1, 0)	$1 + P^2$	1	$1 - P^2$	1
$(1/\sqrt{2}, 1/\sqrt{2})$	1	$1 - P^2$	1	$1 + P^2$
(0, 1)	$1 - P^2$	1	$1 + P^2$	1
$(1/\sqrt{2}, 0) + (0, 1/\sqrt{2})$	1	1	1	1

Let us now turn to a situation in which there are two degenerate Higgs bosons. This can arise in the 2HDM and also in the MSSM. The rates as a function of the relative angle between the transverse polarizations, ζ , will depend in detail upon the \hat{a} and \hat{b} values of the two Higgs bosons. As an example, suppose that we have a degenerate pair at $m_h = 110$ GeV, one of which is pure CP-even with $\hat{a} = 1/\sqrt{2}, \hat{b} = 0$ ($\delta = 0$) and the other pure CP-odd with $\hat{a} = 0, \hat{b} = 1/\sqrt{2}$ ($\delta = \pi/2$). Here, we have chosen the normalizations so that the total unpolarized (i.e. averaged over the four ζ settings) production rate is the same as for a SM Higgs boson, with each of the two Higgs contributing equally to this rate. (We will also assume that the two Higgs bosons have the same $b\bar{b}$ branching ratio as a SM Higgs boson.) In this situation, Eq. (1) shows that the production rate will have no dependence on ζ [$\cos(0 + \zeta) + \cos(\pi + \zeta) = 0$], whereas any single Higgs model will exhibit a distinct pattern as a function of ζ , as illustrated in Table 1. Were we able to accumulate events at fixed ζ , the pattern of $\Delta\chi^2$ for discriminating any two models from one another (assuming all have the same $b\bar{b}$ production rate) is apparent in the approximation where the ζ dependence of the $\Delta N(\zeta)$ errors is neglected (as approximately appropriate given the dominance of the background contribution to ΔN and the weak dependence of the background on ζ); $\Delta\chi^2$ would simply be proportional to the squares of the rate differences between two models summed over the four ζ values. In the case where we compare the ζ -independent rate predicted in a degenerate Higgs pair model to expectations for any given single Higgs boson, it is apparent from the table that the $\Delta\chi^2$ between the degenerate model and *any* single Higgs model is independent of the latter. (This is true for arbitrary δ for a single Higgs since $\cos^2(2\delta) + \cos^2(2\delta + \pi/2) + \cos^2(2\delta + \pi) + \cos^2(2\delta + 3\pi/2) = 2$.)

However, because of spin precession, we must actually employ Eq. (9). Since $\sin 2\delta = 0$ for both Higgs bosons while $\cos 2\delta = 1$ for the CP-even and $\cos 2\delta = -1$ for the CP-odd Higgs boson, after summing over both, the cross section will be

the same as that obtained if we set $\cos 2\delta = 0$ as well as $\sin 2\delta = 0$. To compare to the simplified discussion of the previous paragraph, let us recall that for our choices of configurations and binning we can approximately neglect the C, i, j (i.e. configuration, θ^- and θ) dependence of the $\Delta N(C, i, j)$ denominators in Eq. (21). Then, for the $L/6, L/6, 2L/3$ luminosity weightings for configurations $C = I, C = II, C = III$, respectively, the effective sensitivity for discriminating between the $[\cos 2\delta = \sin 2\delta = 0]$ —equivalent situation for the degenerate pair and the results expected for any single Higgs boson characterized by angle δ will be proportional to $\frac{1}{3}\hat{\mathcal{S}}_a^2 + \frac{2}{3}\hat{\mathcal{S}}_c^2 \sim \frac{1}{3}P^4(\Delta_c^2 + \Delta_s^2) = \frac{1}{3}P^4(\cos^2 2\delta + \sin^2 2\delta) = \frac{1}{3}P^4$ [see Eqs. (18) and (20)], i.e. again independent of the δ value for any single Higgs boson to which one might compare. One finds that this approximation is actually quite good. Taking $L = 0.15 \text{ fb}^{-1}$ for $I = 1$ and $P = 0.2$ and assuming a SM-like $b\bar{b}$ production rate, we find $\Delta\chi^2 =$ (i) 0.38; (ii) 2.8; (iii) 6.4; (iv) 9.8, for the four (I, P) scenarios defined earlier, essentially independent of the type of single Higgs boson exchange to which one compares. Note that we get $\geq 99\%$ CL exclusion of a single Higgs model only for $I > 2$ if nature chooses a degenerate pair. In any case, the ζ dependence is key to separating a degenerate CP-even plus CP-odd pair of Higgs bosons from a single Higgs boson of any given CP nature.

In the MSSM, in the absence of CP violation the most likely situation in which we will encounter a highly degenerate pair of Higgs bosons that cannot be easily separated by scanning in \sqrt{s} is in the limit of large m_{A^0} and large $\tan\beta$. The increasing degeneracy with increasing $\tan\beta$ is illustrated for $m_{A^0} = 400 \text{ GeV}$ in Fig. 6, assuming squark masses of 1 TeV and no squark mixing and a beam energy spread of $R = 0.001$. Since the total widths of the H^0 and A^0 are substantial ($> 1 \text{ GeV}$) for the m_{A^0} and $\tan\beta$ values being considered, it is not guaranteed that we will be able to separate the peaks. The figure shows that we are able to observe two separate peaks (the A^0 peak being at lower mass than the H^0 peak) for moderate $\tan\beta \lesssim 6$. But, for higher $\tan\beta$ values the peaks begin to merge; for $\tan\beta \gtrsim 8$, $|m_{H^0} - m_{A^0}| < 1 \text{ GeV}$ and one sees only a single merged peak. The picture changes if squark mixing is substantial; for instance, for $m_{A^0} = 300 \text{ GeV}$, squark masses of 1 TeV and large squark mixing ($A_t = A_b = 3 \text{ TeV}$), the H^0 and A^0 peaks actually cross at $\tan\beta \sim 5$.

To explore the various possible scenarios, we begin by considering our ability to discriminate between an exactly degenerate pair of CP-even and CP-odd Higgs bosons vs. a single Higgs boson (of a given type) as a function of $\tan\beta$. We note that the present situation is significantly more favorable than that discussed above with a light degenerate pair with SM-like widths, branching ratios and production rate. Since the widths of the H^0 and A^0 are significant, one can operate the muon collider with the natural beam energy resolution of order $R = 0.001$ and still have $\sigma_{\sqrt{s}} < \Gamma$, which maximizes the Higgs production rate.^{#8} At such R and

^{#8}Of course, one could possibly separate the two Higgs bosons by employing $R < 0.0001$, but it is unlikely that the machine would be operated in this way at this higher energy unless a Higgs

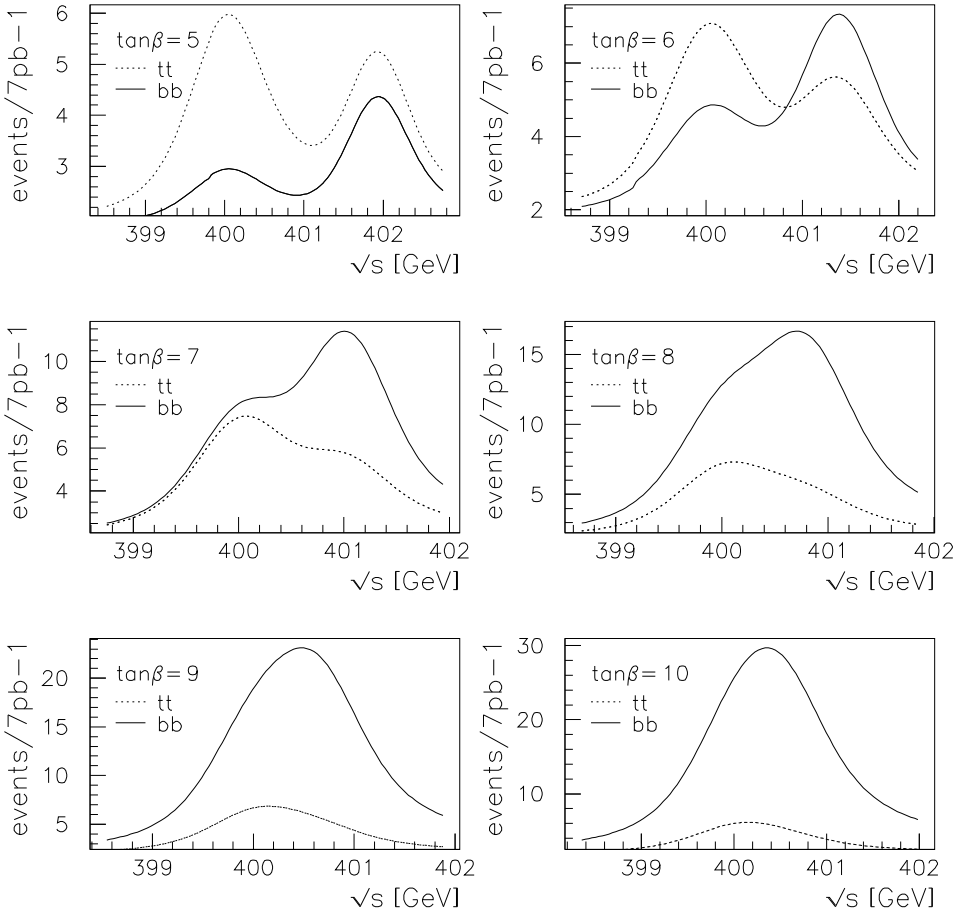


Figure 6: We plot $b\bar{b}$ (solid) and $t\bar{t}$ (dashed) event rates for total integrated luminosity of $L = 7 \text{ pb}^{-1}$ coming from $\mu^+\mu^- \rightarrow H^0 + A^0$ as a function of \sqrt{s} , assuming $m_{A^0} = 400 \text{ GeV}$. Each window is for the specific $\tan\beta$ value noted. These event rates are to be multiplied by a factor of 1000 for the expected yearly integrated luminosity of 7 fb^{-1} . We employ squark masses of 1 TeV and no squark mixing. Supersymmetric decay channels are assumed to be closed.

for $\sqrt{s} \sim 300$ GeV (400 GeV), the nominal yearly integrated luminosity for full bunches at $P = 0.2$ is estimated at $L \sim 2 \text{ fb}^{-1}$ (7 fb^{-1}), i.e. more than a factor of ten larger than the $R = 3 \times 10^{-5}$ value. Second, the $b\bar{b}$ branching ratio for large m_{A^0} and large $\tan\beta$ is inevitably of order 88%, the only significant competitor being $\tau^+\tau^-$. Even for moderate $\tan\beta$ and for Higgs masses above $t\bar{t}$ threshold, the $b\bar{b}$ branching ratio remains substantial. Even more importantly, at large m_{A^0} the $\mu^+\mu^-$ couplings of the H^0 and A^0 are enhanced relative to SM strength by a factor of $\tan\beta$ so that the $\mu^+\mu^-$ branching ratio asymptotes to a constant.

As shown in Figure 6, the H^0 and A^0 need not give exactly the same $b\bar{b}$ event rate (due to differences in $BR(\mu^+\mu^-)BR(b\bar{b})$). This is true even if parameters are chosen so that they are exactly degenerate in mass at some given $\tan\beta$ value. On the other hand, it is also typically possible to choose parameters so that they do have exactly the same rate. We consider this last possibility first. (As already discussed, when the H^0 and A^0 have exactly the same $b\bar{b}$ rate, there is no dependence of the summed $b\bar{b}$ rate on ζ . As a result, even after including spin precession, $\Delta\chi^2$ will be independent of the CP nature of any single Higgs boson to which we compare if we sum over the three configurations $C = I, II, III$ with luminosity weighting $L/6, L/6, 2L/3$.) To simulate this situation, we choose a value of $\tan\beta$ and a value of the A^0 mass. We then compute the H^0 and A^0 event rates (assuming stop masses of 1 TeV and no squark mixing) and reset the H^0 and A^0 event rates so that both are equal to the average of the originally computed H^0 and A^0 rates. We consider m_{A^0} values of 300 GeV and 400 GeV. In the latter case, the $t\bar{t}$ decay channel is open and has significant branching ratio at lower $\tan\beta$ values. This, along with the decreased $\mu^+\mu^-$ coupling at lower $\tan\beta$, is included in computing the $b\bar{b}$ rate. We make no use of the $t\bar{t}$ channel; its inclusion would, of course, increase our discrimination power, especially if the final state correlations that can be probed there are employed. The resulting discrimination power is generally more than adequate without its inclusion.

Figs. 7 and 8 give the results for $m_{A^0} = 300$ GeV (400 GeV), respectively. We plot $\Delta\chi^2$ obtained for the four polarization/proton-source-intensity options (i)-(iv) delineated earlier, but using the higher nominal luminosities stated above: (i) $P = 0.2$, and the $I = 1$ values of $L = 3(10.5) \text{ fb}^{-1}$; (ii) $P = 0.39$, and the $I = 1$ merged-bunch $L = 1.5(5.25) \text{ fb}^{-1}$ values; (iii) $P = 0.48$ and $I = 2$, yielding merged-bunch $L = 1.5(5.25) \text{ fb}^{-1}$; (iv) $P = 0.45$ and $I = 3$, without bunch merging, yielding $L = 3(10.5) \text{ fb}^{-1}$. We emphasize that options (i) and (ii) require no over-design of the proton source. The $\Delta\chi^2$ plots show that good discrimination is obtained even for option (i) once $\tan\beta > 10$. Option (ii) would be needed for good discrimination if $\tan\beta \sim 5$.

We next consider the discrimination power achieved if we continue to enforce

resonance peak is seen and there is already some evidence, through the techniques considered here, that there are actually two overlapping resonances with different CP properties. Even then, there will remain the possibility of very close or even exact degeneracy.

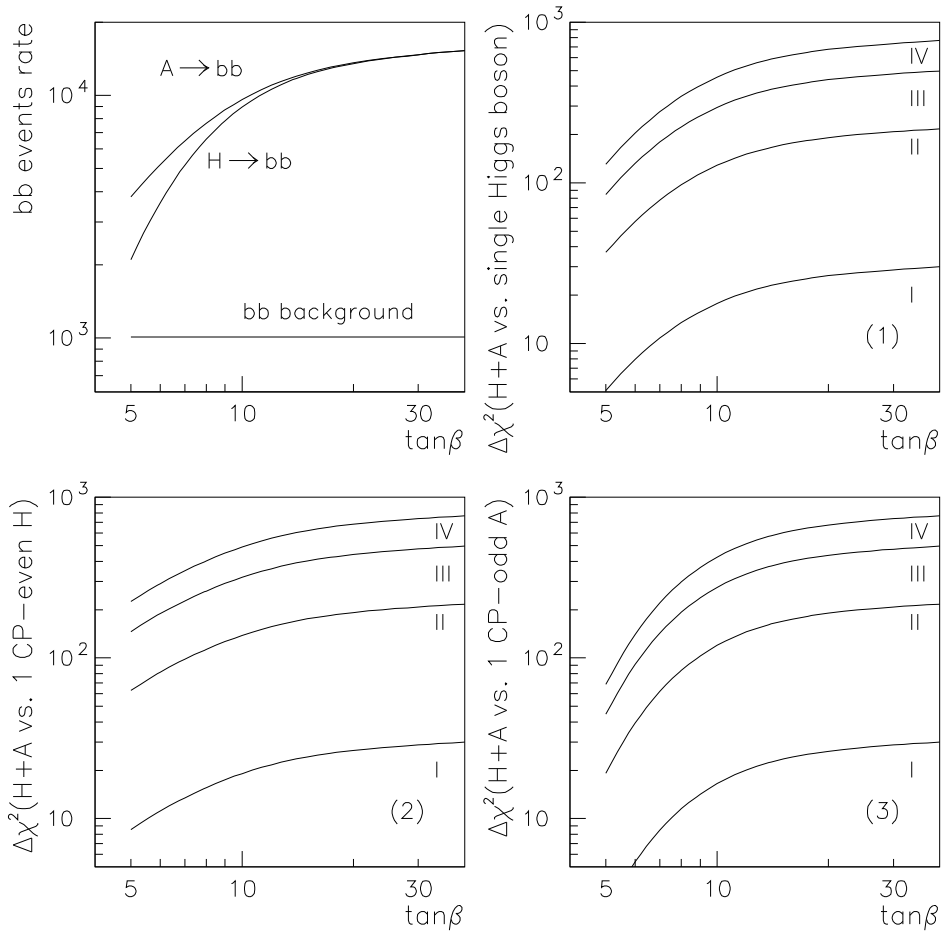


Figure 7: In the upper left window, we plot the $b\bar{b}$ event rates in the MSSM for the H^0 and A^0 (the A^0 rate is the larger of the two) as a function of $\tan\beta$ for $m_{A^0} = 300$ GeV, assuming squark masses of 1 TeV, no squark mixing and integrated luminosity of $L = 2 \text{ fb}^{-1}$. Also shown is the (relatively small) background rate. In the remaining windows we plot $\Delta\chi^2$, after including precession and increasing L to $L = 3 \text{ fb}^{-1}$, as a function of $\tan\beta$ for three different cases in which we forcibly lower m_{H^0} to 300 GeV (for exact degeneracy). (1) We adjust the H^0 and A^0 event rates so that each is exactly equal to the average of the A^0 and H^0 rates as predicted by the MSSM, and compute $\Delta\chi^2$ for $H^0 + A^0$ vs. a single Higgs resonance (of any type) with the same total event rate, employing only the $b\bar{b}$ channel. (2) We use the actual H^0 event rate and compute $\Delta\chi^2$ for $H^0 + A^0$ vs. a single CP-even resonance yielding the same $b\bar{b}$ event rate. (3) As in (2), but vs. a single CP-odd resonance. In cases (1)-(3), we give results as a function of $\tan\beta$ for the four polarization-luminosity situations (i)-(iv) (as labelled on the curves) described in the text.

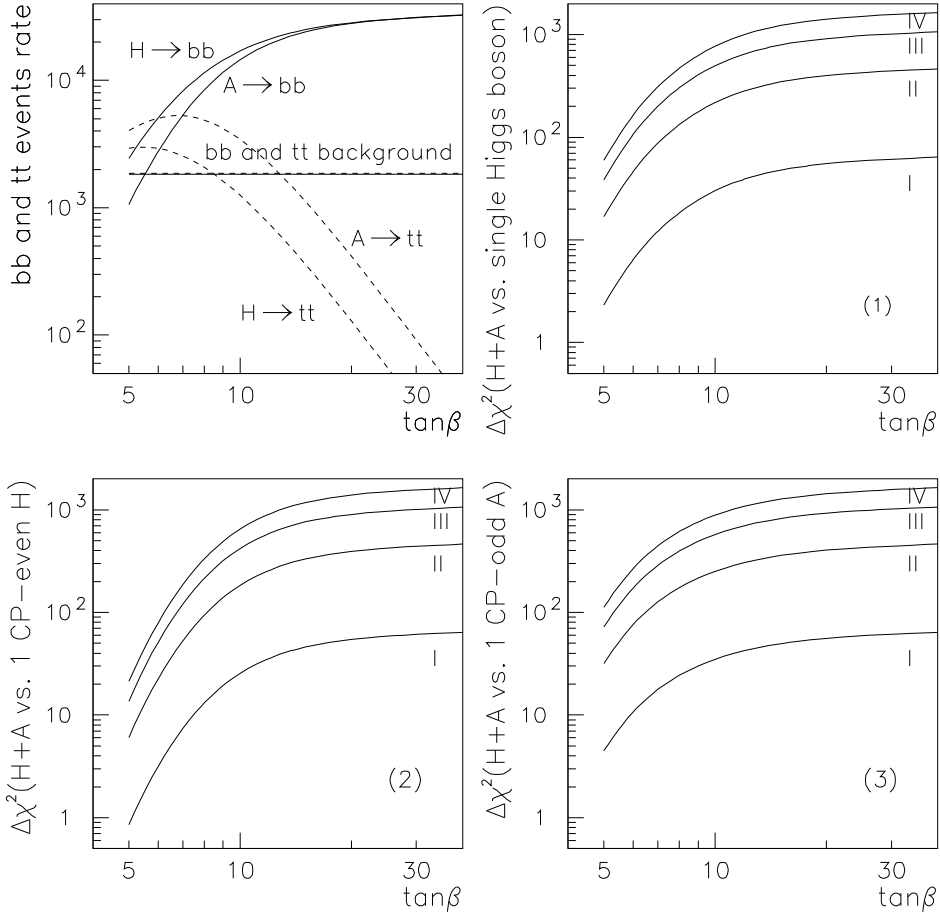


Figure 8: The same as Fig. 7 except for $m_{A^0} = m_{H^0} = 400$ GeV, and using $L = 7 \text{ fb}^{-1}$ for the rate window increased to $L = 10.5 \text{ fb}^{-1}$ for the $\Delta\chi^2$ windows (in order to account for the inefficiency associated with spin precession). The upper-left window gives the H^0 and A^0 and background $t\bar{t}$ event rates as dashed curves. In the $\Delta\chi^2$ analysis, only the $b\bar{b}$ final state (after accounting for the depletion from $H^0, A^0 \rightarrow t\bar{t}$) is employed.

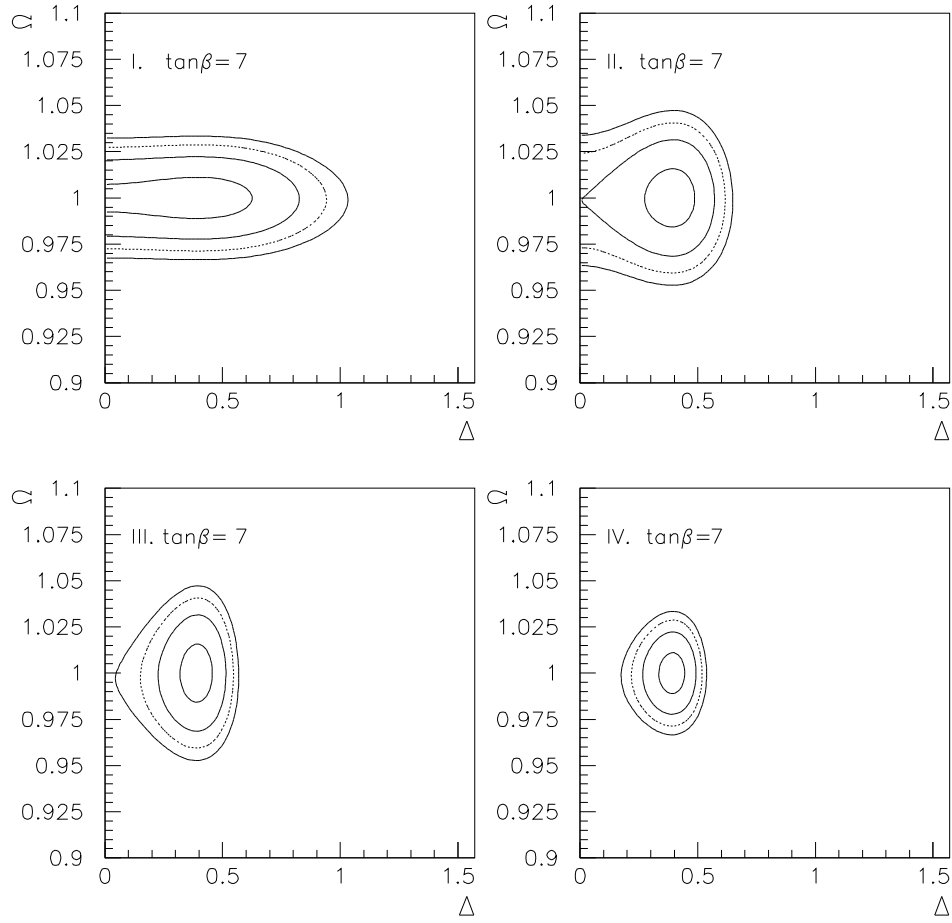


Figure 9: We plot contours of $\Delta\chi^2 = 1, 4, 6.635, 9$ in the Δ, Ω parameter space, assuming $m_{A^0} = 400$ GeV, $\tan\beta = 7$, squark masses of 1 TeV and no squark mixing. The different windows give results for the different proton source intensity and bunch merging options described in the text.

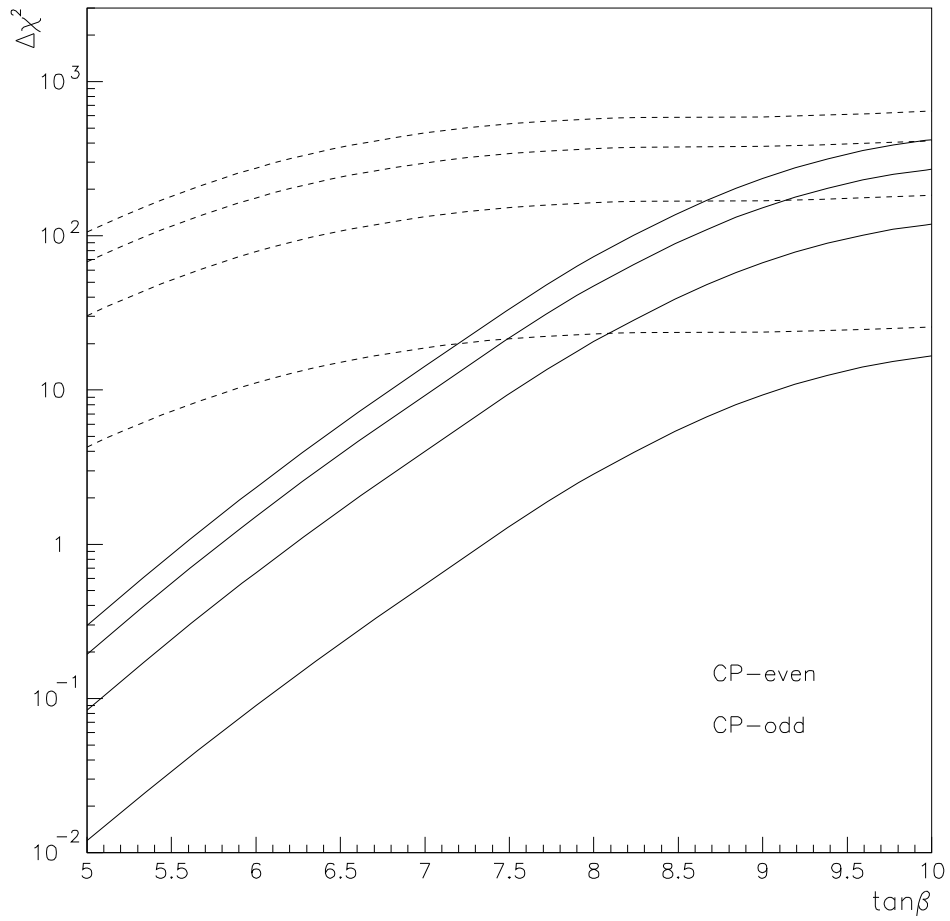


Figure 10: We plot $\Delta\chi^2$ as a function of $\tan\beta$ for discriminating between the $A^0 - H^0$ mixture predicted by the MSSM model (as specified in the text) at $\sqrt{s} = m_{H^0}$ compared to a single CP-even or CP-odd Higgs boson yielding exactly the same $b\bar{b}$ event rate. Results are presented for the polarization/proton-source-intensity options (i)-(iv) described in the text.

exact degeneracy by lowering m_{H^0} to m_{A^0} , but employ the actually predicted A^0 and H^0 event rates. For $m_{A^0} = 300$ GeV, the H^0 event rate for $b\bar{b}$ is lower than the A^0 rate, and the worst (best) discrimination is achieved relative to a purely CP-odd (purely CP-even) Higgs boson (again assumed to have exactly the same total $b\bar{b}$ event rate). The resulting $\Delta\chi^2$ values for options (i)-(iv) are given in the two bottom windows of Fig. 7. Even in the worst case, good discrimination power is achieved for $\tan\beta \geq 5$ by using option (ii). Exactly the reverse situation arises for $m_{A^0} = 400$ GeV. As seen in Fig. 8, the A^0 rate in the $b\bar{b}$ channel is smaller than for the H^0 . Discrimination against a purely CP-even Higgs will be the most difficult. In fact, we see that option (ii) will not provide clear discrimination against a purely CP-even Higgs if $\tan\beta \lesssim 7$.

Finally, let us consider the case where the H^0 and A^0 are not exactly degenerate, but are only nearly so. To be specific we adopt the MSSM predictions of Fig. 6. As noted earlier, if the collider is operated with $R = 0.001$ beam energy spread so as to maximize luminosity, for $\tan\beta \gtrsim 8$ one observes a single broad peak in a scan and we will not know that there are two Higgs bosons present. The apparent peak of the resonance shape will tend to coincide with the mass of the Higgs boson which yields the higher $b\bar{b}$ rate (which Higgs this is depends on the mass, as we have seen). If we center on this apparent peak, the contribution to the $b\bar{b}$ rate from the weaker Higgs will be further reduced because \sqrt{s} is somewhat on the wing of its resonance shape. This further decreases the $\Delta\chi^2$ discrimination power relative to a purely CP-odd (CP-even) Higgs boson if the dominant Higgs is CP-odd (CP-even). Even if we see two separate peaks, we will wish to experimentally determine which is the H^0 and which is the A^0 .

To illustrate, let us define $\Omega = \sqrt{\widehat{N}_{A^0}^2 + \widehat{N}_{H^0}^2}$ and $\Delta = \tan^{-1} \frac{\widehat{N}_{A^0}}{\widehat{N}_{H^0}}$, where \widehat{N}_{A^0} (\widehat{N}_{H^0}) is the number of A^0 (H^0) events at the chosen \sqrt{s} for a possible model divided by $(N_{A^0}^2 + N_{H^0}^2)^{1/2}_{MSSM}$. In Fig. 9, we present $\Delta\chi^2$ contours in Δ, Ω parameter space for the input MSSM model (see Fig. 6) specified by $m_{A^0} = 400$, $\tan\beta = 7$, squark masses of 1 TeV and no squark mixing. To determine that there are A^0 events under the H^0 peak at 99% CL requires the $I = 2$ proton source intensity option (iii). A global overview of our ability to discriminate the MSSM input model from a single purely CP-even (the worst case) or single purely CP-odd (the best case) Higgs boson yielding exactly the same $b\bar{b}$ event rate is provided by Fig. 10. There, we plot $\Delta\chi^2$ for these two discriminations as a function of $\tan\beta$ for polarization/proton-source-intensity options (i)-(iv). We find that discrimination against a purely CP-odd Higgs boson is excellent even for $\tan\beta \sim 5$, whereas $\tan\beta > 9$ [$\tan\beta > 7.3$] is required for 99% CL discrimination against a single CP-even Higgs boson using option (i) [(ii)]. Of course, if squark mixing is large, the degree of degeneracy between the H^0 and A^0 can be such that the peaks will merge even when $\tan\beta \sim 5$. In this case, good discrimination power would typically require enhanced proton source intensity.

5 Summary and Conclusions

The most natural polarization for the muon bunches at a muon collider is $P \sim 0.2$. For this polarization, the collider luminosity will be maximal. In initial exploration of the Higgs or other narrow resonance, one will choose the polarizations to lie in the horizontal plane of the storage ring. As the polarizations rotate it will then be possible to perform a precise measurement of the beam energies and their Gaussian widths and of the degree of polarization itself. Further, by choosing the μ^+ polarization to be 90 degrees out of phase with the μ^- polarization, the effect of the rotating polarization will cancel out when averaging over the 1000 turns during which the typical bunches are stored; i.e. the turn-averaged cross section will be identical to the polarization-averaged cross section. However, once the basic properties of the Higgs boson or resonance are known (total width, branching ratios, etc.) the next important goal will be to determine its CP properties as codified in the relative strength of its scalar and pseudoscalar couplings to fermions. The muon collider provides a perfect opportunity for determining these relative strengths for the muon itself, but only if one has retained the ability to reconfigure the collider so as to run with high polarizations for the muon bunches and to have flexibility in the orientation of these polarizations at the time the bunches are inserted into the storage ring. In most muon collider designs, high polarization can only be achieved by making strong momentum cuts on the muons, which, unless the proton source has ‘spare’ luminosity relative to bunch saturation limits for $P \sim 0.2$, will result in some loss of collider luminosity. However, if the goal is to measure the CP-odd/CP-even coupling ratio, this loss of luminosity is more than compensated by increased sensitivity. Our goal in this paper has been to develop efficient techniques and polarization configurations for determining the CP-odd/CP-even coupling ratio and to quantify the accuracy with which this ratio could be extracted from the data.

We have found that one very effective technique is to accumulate events for three carefully chosen polarization configurations (as defined by the polarization of the μ^+ and μ^- bunches at the time they enter the storage ring). To achieve these three configurations, one will need appropriate solenoids and/or small rings for manipulating the polarizations prior to injection into the storage ring. Once the bunches are in the storage ring, further manipulation would destroy our ability to measure the bunch energies to the 1 part in 10^6 level needed (at least for a narrow Higgs boson). We have demonstrated that by selecting high-polarization muons and performing bunch merging, meaningful constraints on the CP nature of the muonic couplings of a Higgs boson are possible even if it is light and narrow and even if the proton source has only the nominal luminosity required to saturate the bunch limits in the storage ring at relatively low polarization. However, we have seen that extra proton source luminosity (sufficient to saturate the bunch limits of the storage ring when muon selections leading to large polarization are employed) may be needed to achieve a high level of certainty regarding the CP

nature of the muonic couplings of such a Higgs boson. We have also shown that distinguishing a highly degenerate pair of CP-even and CP-odd Higgs bosons from a single Higgs with definite CP nature will generally be possible, especially if this is the degenerate H^0 - A^0 pair of the MSSM at high $\tan\beta$ and large m_{A^0} for which event rates are high and high-luminosity-running at $R = 0.001$ would suffice.

Overall, while the machine capabilities required to make a good determination of the CP nature of the muonic couplings of a Higgs boson do not come without a price, it could well happen that the true nature of an observed Higgs resonance would be obscure without the measurements considered here. Further, Higgs/resonance CP studies provide but one example of how unique sensitivity to new physics can result if we can take advantage of the slow precession of the muon bunch polarizations by manipulating their orientation and relative phases and recording events on a turn-by-turn basis. Thus, we encourage the muon collider designers to retain the flexibilities needed to insert devices for rotating the spins of the beams to a variety of initial (i.e. prior to insertion into the storage ring) configurations of longitudinal and transverse polarization and to consider seriously the possibility of ‘over-designing’ the proton source relative to storage ring bunch saturation limits associated with low polarization. Or, perhaps it will prove possible to employ a very high gradient in the initial phase-rotation stage of pion/muon capture [11, 15, 16], thereby maximizing the luminosity available after the selection cuts required for high polarization.

Acknowledgements

We thank S Geer, R. Raja and R. Rossmanith for helpful conversations on experimental issues. This work was supported in part by the U.S. Department of Energy, the U.C. Davis Institute for High Energy Physics, the State Committee for Scientific Research (Poland) under grant No. 2 P03B 014 14 and by Maria Skłodowska-Curie Joint Fund II (Poland-USA) under grant No. MEN/NSF-96-252. Two of the authors (BG, JP) are indebted to the U.C. Davis Institute for High Energy Physics for the great hospitality extended to them while this work was being performed.

6 Appendix

In this appendix, we present the analytic formulae for the signal and background cross sections in an arbitrary fermionic final state. Fermionic couplings take the form $i\gamma_\mu e_f$ (photon), $i\gamma_\mu(c_f+d_f\gamma_5)$ (Z), and $i(a_f+i\gamma_5b_f)$ (Higgs). Here, $e_f = eQ_f$, $c_f = \frac{g}{2\cos\theta_W}(T_3^f - 2Q_f\sin^2\theta_W)$, $d_f = -\frac{g}{2\cos\theta_W}T_3^f$, and, for a SM Higgs boson, $a_f = \frac{gm_f}{2m_W}$ and $b_f = 0$. In terms of these quantities, the decay width of the Higgs

boson to $f\bar{f}$ is given by

$$\Gamma(h \rightarrow f\bar{f}) = \frac{1}{8\pi} \beta_f m_h (a_f^2 \beta_f^2 + b_f^2), \quad (22)$$

$$\text{where } \beta_f \equiv \sqrt{1 - \frac{4m_f^2}{s}}.$$

We employ the center of mass system with $\sqrt{s} = E_{\text{CM}}$ and define $\zeta \equiv \zeta^+ - \zeta^-$ as the angle of the μ^+ transverse polarization relative to that of the μ^- . The explicit expressions for the 4-momenta and spin vectors of the μ^+ and μ^- in the laboratory frame are:

$$\begin{aligned} p_{\mu^-} &= \frac{\sqrt{s}}{2} (1, 0, 0, \beta) \\ p_{\mu^+} &= \frac{\sqrt{s}}{2} (1, 0, 0, -\beta) \\ s_{\mu^-} &= P_L^- \gamma(\beta, 0, 0, 1) + P_T^- (0, \cos \zeta^-, \sin \zeta^-, 0) \\ s_{\mu^+} &= P_L^+ \gamma(\beta, 0, 0, -1) + P_T^+ (0, \cos \zeta^+, \sin \zeta^+, 0) \\ p_f &= \frac{\sqrt{s}}{2} (1, \beta_f \sin \theta \cos \phi, \beta_f \sin \theta \sin \phi, \beta_f \cos \theta) \\ p_{\bar{f}} &= \frac{\sqrt{s}}{2} (1, -\beta_f \sin \theta \cos \phi, -\beta_f \sin \theta \sin \phi, -\beta_f \cos \theta), \end{aligned} \quad (23)$$

where ϕ and θ are the standard angles defined using polar coordinates for the final fermion. The forms for s_{μ^-} and s_{μ^+} above are those which make the separation between longitudinal and transverse polarization most evident. The conversion between these forms and those given earlier in Eqs. (7) and (8) appropriate to making the precession physics most transparent can be accomplished by the following mappings:

$$P_H^\pm \cos \theta^\pm = P_L^\pm, \quad -P_H^\pm \sin \theta^\pm = P_T^\pm \cos \zeta^\pm, \quad P_V^\pm = P_T^\pm \sin \zeta^\mp. \quad (24)$$

We now give expressions for the invariant matrix element squared, $|\mathcal{M}|^2$, for $\mu^+ \mu^- \rightarrow f\bar{f}$, summed over final spins and averaged over initial spins. These will be given in terms of P_L^\pm , P_T^\pm and ζ^\pm . Eq. (24) can be used to convert to the P_H^\pm , P_V^\pm and θ^\pm precession variables. We divide $|\mathcal{M}|^2$ into three pieces: the absolute square of the Higgs diagram, the interference between the Higgs diagram and the $\gamma^* + Z^*$ exchange background diagrams, and the absolute square of the $\gamma^* + Z^*$ background diagrams. The symbols \Re and \Im denote the real and imaginary parts. We give the results for $m_\mu/\sqrt{s} \rightarrow 0$, an excellent approximation for any reasonable Higgs mass. Defining $\Pi_X \equiv [s - m_X^2 + i\Gamma_X m_X]^{-1}$ we have the following.

Absolute square of Higgs exchange:

$$\begin{aligned} & (a_f^2 \beta_f^2 + b_f^2) |\Pi_h|^2 s^2 \left[(a_\mu^2 + b_\mu^2) (1 + P_L^- P_L^+) + P_T^- P_T^+ \left\{ (a_\mu^2 - b_\mu^2) \cos \zeta - 2 a_\mu b_\mu \sin \zeta \right\} \right] \\ &= (a_f^2 \beta_f^2 + b_f^2) |\Pi_h|^2 s^2 (a_\mu^2 + b_\mu^2) \left[(1 + P_L^- P_L^+) + P_T^- P_T^+ \cos(\zeta + 2\delta) \right] \end{aligned} \quad (25)$$

Higgs $- \gamma^* + Z^*$ Interference:

$$\begin{aligned}
& 4 \sin \theta a_f (a_\mu^2 + b_\mu^2)^{1/2} m_f \beta_f s^{3/2} \left\{ \right. \\
& - \sin(\zeta^+ + \delta - \phi) P_T^+ \left[e_f e_\mu \Im(\Pi_\gamma \Pi_h^*) + c_f (c_\mu + d_\mu P_L^-) \Im(\Pi_Z \Pi_h^*) \right] \\
& - \sin(\zeta^- - \delta - \phi) P_T^- \left[e_f e_\mu \Im(\Pi_\gamma \Pi_h^*) + c_f (c_\mu - d_\mu P_L^+) \Im(\Pi_Z \Pi_h^*) \right] \\
& - \cos(\zeta^+ + \delta - \phi) P_T^+ \left[e_f e_\mu P_L^- \Re(\Pi_\gamma \Pi_h^*) + c_f (c_\mu P_L^- + d_\mu) \Re(\Pi_Z \Pi_h^*) \right] \\
& \left. + \cos(\zeta^- - \delta - \phi) P_T^- \left[e_f e_\mu P_L^+ \Re(\Pi_\gamma \Pi_h^*) + c_f (c_\mu P_L^+ - d_\mu) \Re(\Pi_Z \Pi_h^*) \right] \right\} \\
\end{aligned} \tag{26}$$

Absolute square of $\gamma^* + Z^*$:

$$\begin{aligned}
& -8 d_f^2 \left[(c_\mu^2 + d_\mu^2) (1 - P_L^- P_L^+) + 2 c_\mu d_\mu (P_L^- - P_L^+) \right] m_f^2 |\Pi_Z|^2 s \\
& + 2 \sin(\zeta - 2\phi) \sin^2 \theta P_T^- P_T^+ c_f d_\mu e_f e_\mu \Im(\Pi_Z) \Pi_\gamma \beta_f^2 s^2 \\
& + \cos(\zeta - 2\phi) \sin^2 \theta P_T^- P_T^+ \left\{ (c_f^2 + d_f^2) (c_\mu^2 - d_\mu^2) |\Pi_Z|^2 + e_f^2 e_\mu^2 \Pi_\gamma^2 + 2 e_f e_\mu c_f c_\mu \Pi_\gamma \Re(\Pi_Z) \right\} \beta_f^2 s^2 \\
& + (2 - \beta_f^2 \sin^2 \theta) \left\{ (c_f^2 + d_f^2) \left[(c_\mu^2 + d_\mu^2) (1 - P_L^- P_L^+) + 2 c_\mu d_\mu (P_L^- - P_L^+) \right] |\Pi_Z|^2 \right. \\
& + 2 c_f e_f e_\mu \left[c_\mu (1 - P_L^- P_L^+) + d_\mu (P_L^- - P_L^+) \right] \Pi_\gamma \Re(\Pi_Z) + e_f^2 e_\mu^2 (1 - P_L^- P_L^+) \Pi_\gamma^2 \left. \right\} s^2 \\
& + 4 \cos \theta d_f \left\{ c_f \left[2 c_\mu d_\mu (1 - P_L^- P_L^+) + (c_\mu^2 + d_\mu^2) (P_L^- - P_L^+) \right] |\Pi_Z|^2 \right. \\
& \left. + e_f e_\mu \left[d_\mu (1 - P_L^- P_L^+) + c_\mu (P_L^- - P_L^+) \right] \Pi_\gamma \Re(\Pi_Z) \right\} \beta_f s^2
\end{aligned} \tag{27}$$

In terms of $|\mathcal{M}|^2$, the cross section as a function of s , θ and ϕ is given by

$$\frac{d\sigma}{d \cos \theta d\phi} = \frac{1}{64\pi^2 s} \beta_f |\mathcal{M}|^2. \tag{28}$$

For example, if we spin average the Higgs portion of $|\mathcal{M}|^2$ by combining $\zeta = 0$ and $\zeta = \pi$ (so that the average of $\cos \zeta$ is zero), integrate over $d \cos \theta$ and $d\phi$, and use Eq. (22), then we obtain the standard spin-averaged total cross section: $\sigma(s) = 4\pi \Gamma(h \rightarrow \mu^+ \mu^-) \Gamma(h \rightarrow f\bar{f}) |\Pi_h|^2$. When this latter form is convoluted with a Gaussian distribution in \sqrt{s} , one obtains the result of Eq. (2).

References

[1] For a review and references, see: J.F. Gunion, H.E. Haber, G. Kane and S. Dawson, *The Higgs Hunters Guide* (Addison-Wesley Publishing Company, Redwood City, CA, 1990).

- [2] T.D. Lee, *Phys. Rev.* **D8** (1973) 1226; S. Weinberg, *Phys. Rev.* **D42** (1990) 860.
- [3] A. Pilaftsis, *Phys. Rev.* **D58** (1998) 096010, *Phys. Lett.* **B435** (1998) 88; D.A. Demir, *Phys. Rev.* **D60** (1999) 055006.
- [4] R. Casalbuoni, A. Deandrea, S. De Curtis, D. Dominici, R. Gatto, and J.F. Gunion, *Nucl. Phys.* **B555** (1999) 3.
- [5] B. Grzadkowski and J.F. Gunion, *Phys. Lett.* **B350** (1995) 218.
- [6] D. Atwood and A. Soni, *Phys. Rev.* **D52** (1995) 6271.
- [7] J.F. Gunion, B. Grzadkowski, X.-G. He, *Phys. Rev. Lett.* **77** (1996) 5172, hep-ph/9605326; J.F. Gunion and J. Pliszka, *Phys. Lett.* **B444** (1998) 136, hep-ph/9809306; B. Grzadkowski and J. Pliszka, *Phys. Rev.* **D60** (1999) 115018, hep-ph/9907206.
- [8] B. Grzadkowski and J.F. Gunion, *Phys. Lett.* **B294** (1992) 361, hep-ph/9206262.
- [9] V. Barger, M.S. Berger, J.F. Gunion and T. Han, *Phys. Rept.* **286**, 1 (1997), hep-ph/9602415. *Phys. Rev. Lett.* **75** (1995) 1462, hep-ph/9504330.
- [10] J.F. Gunion, Proceedings of the Workshop on ‘Physics at the First Muon Collider and at the Front End of the Muon Collider’, Batavia, IL, 6-9 Nov 1997, p. 37, hep-ph/9802258. Proceedings of the 5th International Conference on Physics Beyond the Standard Model, Balholm, Norway, 29 Apr - 4 May 1997, p. 234, hep-ph/9707379.
- [11] C.M. Ankenbrandt *et al.*, *Phys. Rev. ST Accel. Beams* **2**, 081001 (1999).
- [12] “Prospective Study of Muon Storage Rings at CERN”, edited by B. Autin, A. Blondel and J. Ellis (CERN 99-02, ECFA 99-197).
- [13] V. Bargmann, L. Michel and V.L. Telegdi, *Phys. Rev. Lett.* **2** (1959) 435.
- [14] R. Raja and A. Tollestrup, private communication.
- [15] D.M. Kaplan, Fermilab-Conf-00/019.
- [16] We thank S. Geer for providing details regarding this option.